HHS Public Access

Author manuscript

J Toxicol Environ Health B Crit Rev. Author manuscript; available in PMC 2023 July 04.

Published in final edited form as:

J Toxicol Environ Health B Crit Rev. 2022 July 04; 25(5): 211–249.

doi:10.1080/10937404.2022.2092569.

Identification of effective control technologies for additive manufacturing

Johan du Plessis[a], **Sonette du Preez**[a], **Aleksandr B. Stefaniak**[b]

[a]Occupational Hygiene and Health Research Initiative, North-West University, Potchefstroom, South Africa

[b]Respiratory Health Division, National Institute for Occupational Safety and Health, Morgantown, WV, USA

Abstract

Additive manufacturing (AM) refers to several types of processes that join materials to build objects, often layer-by-layer, from a computer-aided design file. Many AM processes release potentially hazardous particles and gases during printing and associated tasks. There is limited understanding of the efficacy of controls including elimination, substitution, administrative, and personal protective technologies to reduce or remove emissions, which is an impediment to implementation of risk mitigation strategies. The Medline, Embase, Environmental Science Collection, CINAHL, Scopus, and Web of Science databases and other resources were used to identify 42 articles that met the inclusion criteria for this review. Key findings were as follows: 1) engineering controls for material extrusion-type fused filament fabrication (FFF) 3-D printers and material jetting printers that included local exhaust ventilation generally exhibited higher efficacy to decrease particle and gas levels compared with isolation alone, and 2) engineering controls for particle emissions from FFF 3-D printers displayed higher efficacy for ultrafine particles compared with fine particles and in test chambers compared with real-world settings. Critical knowledge gaps identified included a need for data: 1) on efficacy of controls for all AM process types, 2) better understanding approaches to control particles over a range of sizes and gas-phase emissions, 3) obtained using a standardized collection approach to facilitate inter-comparison of study results, 4) approaches that go beyond the inhalation exposure pathway to include controls to minimize dermal exposures, and 5) to evaluate not just the engineering tier, but also the prevention-through-design and other tiers of the hierarchy of controls.

Keywords

Ultrafine particles; particle emission; volatile organic compounds; indoor air quality; filtration

CONTACT Johan du Plessis, Johan.DuPlessis@nwu.ac.za, Occupational Hygiene and Health Research Initiative, North-West University, Private Bag X6001, Potchefstroom 2520, South Africa.

Supplemental data for this article can be accessed online at https://doi.org/10.1080/10937404.2022.2092569

Disclosure statement

No potential conflict of interest was reported by the author(s)

Introduction

Additive manufacturing (AM) is a broad term for several types of processes that join materials to build objects from a computer-aided design file, often using layer-by-layer methodology. Based upon harmonized terminology, there are seven basic AM process categories: binder jetting (BJ), directed energy deposition (DED), material extrusion (ME), material jetting (MJ), powder bed fusion (PBF), sheet lamination (SL), and vat photopolymerization (VP) (ISO/ASTM 2015). Details on the principles of operation and/or feedstock materials used in each process category are described in recent reviews (Chen et al. 2020; Stefaniak, Du Preez, and Du Plessis 2021a; Zhang et al. 2018). With the exception of SL, for which there are no apparent monitoring data available, it is well established that potentially hazardous particles and gases are emitted throughout AM processes including pre-printing, printing, post-printing, and/or post-processing tasks, which may result in occupational exposures (Aluri et al. 2021; Chan et al. 2020; Leso et al. 2021; Stefaniak, Du Preez, and Du Plessis 2021a).

For AM, the primary exposure pathways are the dermal and inhalation routes. The relative risk for each route varies with the process category and feedstock material. Allergic contact dermatitis was observed among VP and MJ process workers who had skin contact with liquid photopolymer resin feedstocks (Chan et al. 2018; Chang et al. 2004; Creytens et al. 2017). A case of work-related asthma was attributed to the inhalation of emissions from several ME-type fused filament fabrication (FFF) 3-D printers operating simultaneously with acrylonitrile butadiene styrene (ABS) feedstock (House, Rajaram, and Tarlo 2017). In a questionnaire survey of AM workers, 27/46 (59%) of participants responded that they experienced respiratory symptoms at least once per week in the past year and individuals who worked for >40 hr/week with AM machines were significantly more likely to report a previous respiratory-related diagnosis including asthma or allergic rhinitis (Chan et al. 2018). In contrast to these observations, Gumperlein et al. (2018) detected no significant changes in spirometry or nasal and urinary inflammatory biomarkers, though there was a significant difference in the time course of exhaled nitric oxide, when healthy adults in a single-blinded, randomized, crossover design were exposed to emissions from a ME-type FFF 3-D printer using ABS or polylactic acid (PLA) feedstocks for one hr.

Multiple lab toxicology studies evaluated the toxicity of emissions from ME-type FFF 3-D printers. Rats that inhaled emissions during printing with ABS feedstock for one hr developed acute hypertension and microvascular dysfunction (Stefaniak et al. 2017a). Emissions from ABS and polycarbonate feedstock induced concentration-dependent significant cytotoxicity, oxidative stress, apoptosis, necrosis, and production of pro-inflammatory cytokines and chemokines in human small airway epithelial cells *in vitro* (Farcas et al. 2019). In a follow-on study using the same ABS feedstock, rats exposed via inhalation to printing emissions developed transient pulmonary and systemic toxicity (Farcas et al. 2020). Emissions from printing with PLA feedstock significantly reduced the viability of human tumorigenic bronchial epithelial cells (A549) and rat alveolar macrophages (NR8383) cells *in vitro*, and emissions from printing with PLA and ABS feedstocks produced a significant inflammatory response in mice (Zhang et al. 2019). In a study of 3-D pens, which are handheld extruders that operate similar to FFF 3-D printers, the toxicity of

emissions from PLA filament with or without copper, steel, and carbon nanotube additives were tested using A549 cell *in vitro*; only the PLA-copper filament induced adverse effects, which included higher changes in stress, cell death, and metabolic perturbations (Singh et al. 2021). In the only study of the toxicity of BJ emissions, A549 cells and BEAS-2B bronchial epithelial cells were directly exposed to particles from printing with stainless steel powder feedstock; no significant alterations in cell viability and in intracellular reactive oxygen species (ROS) were reported for both cell types (Lewinski, Secondo, and Ferri 2019). Condensate/spatter particles formed during a PBF process with five different metal alloy powders, including steel, nickel alloys, and a titanium alloy, induced low cytotoxicity, genotoxicity, and induction of inflammatory responses in human bronchial epithelial cells *in vitro* (Vallabani et al. 2022).

Several toxicology studies demonstrated that objects built using AM processes might induce adverse effects. Popov et al. (2004) reported that VP printed implants induced significant inflammation at implantation sites in rats. Ecotoxicology studies demonstrated that AM printed objects initiated various adverse effects in zebrafish (De Almeida et al. 2018; Macdonald et al. 2016; Oskui et al. 2016).

Collectively, existing exposure and toxicology data support the potential for risk during work with some AM processes and feedstocks. Risk assessment approaches account for the probability of an adverse effect occurring (exposure) and the severity of an adverse health effect (hazard) (Dugheri et al. 2022; Petretta et al. 2019). When conducting risk assessments, factors related to exposure include, but are not limited to, particle size (where the particle might be deposited in the respiratory tract) and frequency of events (amount of material used for a task and number of times exposure occurs). Factors related to hazard include toxicity including carcinogenicity or reproductive effects and type of response such as acute, chronic, reversible, or irreversible. As such, risk-based selection of control technologies is necessary to ensure greater risk control for certain tasks such as handling toxic metal powder feedstock for PBF processes compared with handling solid polymer feedstock for ME processes. When implementing controls, health and safety professionals often rely on the "hierarchy of controls" One representation of the hierarchy depicts elimination, substitution, engineering controls, administrative controls, and personal protective equipment (PPE) as an inverted triangle, with the most effective control options listed at the top and the least effective options listed at the bottom (NIOSH 2015). Prevention-through-design (PtD), sometimes termed safe-by-design, is a complementary health and safety management methodology that aims to anticipate and design out hazards at the early stages of facility, work operations, process, equipment, tools, and product development (Karayannis et al. 2019). PtD effectively transcends all control types, and thus for purposes of this review, as illustrated in Figure 1, in our version of the hierarchy, it is the most effective option depicted.

Since the first report of particle emissions from ME-type FFF 3-D printers by Stephens et al. (2013), there have been numerous recommendations for implementation of controls; however, investigations of the efficacy of controls are scarce. Further, published studies utilized a range of instruments and metrics to evaluate emissions from AM processes as summarized herein, which in turn, limited the availability of directly comparable data for

a given instrument and metric on efficacy of controls. An in-depth discussion of particle measurement instrumentation and metrics is beyond the scope of this review; however, for context, a brief overview of these topics is provided in the Supplemental File.

A critical knowledge gap is to understand which controls are effective in capturing emissions from each AM process category as a prerequisite for risk assessment and mitigation. The purposes of this review were to (1) identify literature on tested controls for AM process emissions and (2) critically evaluate their effectiveness with the goal of summarizing the current state of knowledge for health and safety professionals.

Methods

For the purposes of this review, criteria for inclusion were as follows: 1) peer-reviewed journal article or Government report in the English language, 2) control that was specific for an AM process, 3) control that was quantitatively evaluated, 4) tests were performed in a workplace, room (including offices, closets, or labs), or test chamber (a box surrounding a printer to isolate the machine from its environment) setting, and 5) the report included a measure (or data) to quantify effectiveness. Exclusion criteria were as follows: 1) non-peer reviewed magazine articles, book chapters, conference abstracts, and dissertations, 2) controls not specific to AM processes, 3) recommended controls that were not tested, 4) no description of the test environment, and 5) qualitative outcomes including statements such as “appeared” or “seemed” to lower emissions.

Information sources

Identification of potentially relevant literature began with inspection of AM-related articles that the authors had on file. Keywords from these articles were compiled to develop a list of terms for database searching. These terms were grouped into three strings that were combined using the Boolean operator AND for database searches. The first string was synonyms and variations of “additive manufacturing” the second string was terms related to emissions and exposures, and the third string was terms related to control technologies. The combined search string is given in the supplemental file. Supplemental Figure S1 gives the disposition of published articles identified by the database searches. A total of 42 published papers were identified that met our inclusion criteria for this review.

Data analysis

Multiple types of instruments were used in the included papers to monitor particle emissions. These instruments generally detect particles in different size ranges, which limited our ability to make direct comparisons of concentration values. As such, we calculated efficacy as a percentage, which gives a unitless number that can be compared across instruments and studies. Efficacy of a control was calculated (if not already presented in an article) using the general formula $E = \frac{(X - Y)}{X} * 100$. For example, in studies of the efficacy of a ventilation control, X = concentration in a space with ventilation off and Y = concentration in the space with ventilation on; in investigations of the efficacy of a machine cover isolation control, X = concentration in the space with the cover off and Y = concentration in the space with the cover on; in investigations of distance as an

administrative control, X = concentration near an AM machine and Y = concentration further from the machine.

Efficacy values for particle- and gas-phase emissions and contextual information extracted from published papers (Table 1) were imported into JMP statistical software (v13.2.0, SAS Institute Inc., Cary, NC) to calculate median efficacy values for descriptive comparisons. No attempt was made to perform statistical tests of the efficacy data. Preprinting, post-printing, and post-processing task data were excluded from summarization because there were few data points for these tasks and the nature of these tasks might necessitate different work configurations and control designs than for printers. For particle emissions during printing, 148 values on efficacy of controls were extracted from published papers (ME = 139, MJ = 6, PBF = 2, and BJ = 1). Approximately 94% (139/148) of these efficacy values were for the ME process category. More specifically, 92% (128/139) of data were specific to FFF 3-D printers, so detailed inspection of efficacy of controls for particles were limited to this single type of machine. To further reduce variability, 15 mass- and 9 surface-area-based efficacy values were excluded, which left 104 number-based efficacy values (any instrument) to calculate medians. Multiple studies in Table 1 demonstrated that, under the specific room conditions evaluated, general exhaust ventilation (GEV) was ineffective to control particle emissions from ME-type FFF 3-D printers (Secondo et al. 2020; Viitanen et al. 2021). After the exclusion of 10 GEV data points for FFF 3-D printers, there were 94 number-based efficacy values (any instrument) available for summary inspection. For gas-phase emissions during printing, 68 values on efficacy of controls were extracted from published papers (ME = 41, MJ = 23, and VP = 4). Given the small numbers of efficacy values available for VP printers (n = 4) and ME-type large-format printers (n = 4), both were excluded from more detailed analyses. In addition, two efficacy values reported for MJ printers were summations of carbonyl compounds, which were neither a measure of individual VOC concentration nor TVOC concentration, and these were excluded from analyses. The net result was 58 values on the efficacy of controls for gas-phase emissions (37 for ME-type FFF 3-D printers and 21 values for MJ printers).

Results

Figure 1 summarizes the number of articles included in this review and are organized by our version of the hierarchy of controls. No literature was identified on the use of controls for the SL process category. Table 1 provides details of the literature on controls for the remaining 6 AM process categories and is organized by our version of the hierarchy.

Prevention-through-design

The PtD principles are a set of strategies aimed at eliminating exposures and minimizing risks prior to application of materials or products is implemented (i.e., in the conceptualization and design stages). MacCuspie et al. (2021) reported that computational fluid dynamics (CFD) modeling in conjunction with measurement of particle emission rates contributed to the proactive design of workspaces. CFD modeling was used to characterize the dispersion of particles in a space. The experimental procedure consisted of measuring particle emissions from an ME-type FFF 3-D printer with an open-frame design inside a test

chamber that was positioned inside a Class 1000 clean room. The test chamber was outfitted with an air exchange intake, air exchange vent, and three ports fitted with a scanning mobility particle sizer (SMPS), optical particle sizer (OPS), and a cyclone connected to a sampling pump, respectively. The particle emission rate profile of the FFF 3-D printer in the test chamber was used as input data for CFD modeling. Next, the Class 1000 clean room (without test chamber) was utilized as a simulated printing environment. Eight selected locations within the clean room were used to measure particle emissions from the FFF 3-D printer and compared to the CFD modeled results. The CFD prediction met all criteria point for airborne dispersion modeling, which indicated that experimental findings that were obtained aligned with the CFD model predictions. SMPS monitoring data indicated a maximum particle concentration of 1×10^4 #/cm^3 and calculated an average emission rate of 4.85×10^{10} #/min during the printing phase. Based upon their results, MacCuspie et al. (2021) concluded that forced clean airflows in a space might lower particle levels. An advantage of combining CFD modeling with experimental data was that it provided a better understanding of particle levels in areas utilizing FFF 3-D printers. Further, modeling may be employed as a cost-effective approach without having to replicate physical experiments and contribute to the preemptive design of controls specific to workplace conditions.

Elimination controls

No data were identified in the literature on the use of elimination controls for any AM process category.

Substitution controls

This control category occupies the third tier in our version of the hierarchy of controls (Figure 1). Two studies evaluated emissions from ME-type FFF 3-D printers using filaments made from recycled and virgin plastics. The first studymonitored particle- and gas-phase emissions while printing with PLA and ABS filaments at two temperatures (Stefaniak et al. 2021b). For PLA, two recycled filaments made from waste 3-D prints were used, one had green color, the other was gray. From fast mobility particle sizer (FMPS) measurements, it was found that under the “hot” print condition, relative to virgin PLA filament, the recycled green and gray PLA filaments emitted more particles (−89.2 and −39.3% effectiveness, respectively). Under “normal” and “hot” print conditions, relative to virgin ABS filament, the recycled ABS filament emitted less particles (15.9% and 56.7% effectiveness, respectively). Compared with their respective virgin filaments, all recycled filaments emitted lower total volatile organic compound (TVOC) concentrations (range: 24.6% to 55.5%). Väisänen et al. (2021) evaluated virgin and recycled PLA filaments and virgin polypropylene (PP) filament that were purchased from commercial vendors and a recycled PP filament they made from water bottle caps. These investigators printed three tensile test specimens with each filament, shredded any unused filament, extruded it into filament, and printed three more test specimens; this process was repeated up to 5 times (termed “thermal cycles” (TC)). Emissions were monitored using a condensation nuclei counter (CNC). For PLA, relative to virgin plastic, over 5 TCs, the recycled filament generally emitted 1.2% to 45.0% fewer particles. For PP, relative to virgin plastic, over three TCs, the recycled filament emitted more particles (i.e., effectiveness was −129.3% at baseline and −775.3% after the third TC).

Engineering controls

This category occupies the fourth tier in our version of the hierarchy of controls and was the tier for which the majority of evaluations focused to reduce AM process emissions (Figure 1). For purposes of this review, engineering controls were classified as (1) ventilation, e.g., local exhaust ventilation (LEV) or dilution/GEV; (2) isolation, e.g., non-ventilated enclosures; and (3) ventilated enclosures, e.g., enclosure with LEV. In some cases, an engineering control was incorporated into the AM machine design by the manufacturer, and in other cases, it was retrofit to the machine.

Ventilation

No report of ventilation controls for BJ, VP, PBF, or DED machines was identified by the literature search. Väisänen et al. (2022) noted a LEV control for an MJ machine and 6 articles evaluated ventilation controls for ME-type FFF 3-D printers. Of these six articles, three evaluated LEV at or near to the extruder nozzle (Dunn et al. 2020; Kwon et al. 2017; Viitanen et al. 2021), one evaluated the efficacy of a room LEV system (Zontek, Scotto, and Hollenbeck 2021), one evaluated the efficacy of an air purifier equipped with different particulate and gas combination filters positioned near a printer (Gu et al. 2019), and one evaluated room GEV (Secondo et al. 2020).

Väisänen et al. (2022) measured particles, VOCs, and carbonyls emitted from an MJ printer. The printer had a built-in LEV duct, and samples were collected from the lab room air and from the printer exhaust ventilation duct (operating at 7 ACH) when using different resins. Most noteworthy was the distinction made between emissions from a VeroBlackPlus ink-like resin (henceforth, black) and other resins (a combination of clear, white, magenta, cyan, and yellow, henceforth, multi). Compared with room levels during printing, the LEV system was efficient in removing 62.1% (multi) to 68.6% (black) of particles measured using a CNC, 97.6% (multi) to 96.8% (black) of TVOC, and 44.2% (multi) to 57.9% (black) of carbonyls. Individual VOCs were removed with an efficacy of up to 98.9% (isobornyl alcohol, black). The removal of individual carbonyls ranged from 35.3% (formaldehyde, black) to 75.0% (acetone and propionaldehyde, black; 2-butanone, multi).

Kwon et al. (2017) studied multiple retrofit control options to reduce ultrafine particle (UFP; $d < 100$ nm) emissions from a ME-type FFF 3-D printer. Among the options was a suction fan (speed of 6000 revolutions per min, flow rate of 2.7×10^{-4} m^3/s, and face velocity of 0.2 m/s) with activated carbon filter placed horizontally in front of the extruder. Background-corrected SMPS measurements indicated that, relative to the printer operating with no controls, this ventilation suction fan control measure was ineffective and led to an increase in UFPs in the test chamber (efficacy of −38.9%). The ineffectiveness was attributed to the suction fan placement only to the front rather than surrounding the extruder nozzle, which created turbulent flow around the extruder nozzle, with a low flow rate of suction. Several other control options from the study by Kwon et al. (2017) are described in the ventilated enclosure section below. In a study by Dunn et al. (2020) the detachable Smart Extruder of a MakerBot Replicator+ (ME-type FFF 3-D printer) was removed and the existing plastic cover that supplied cooling air to the extruder from three directions and replaced with a NIOSH-designed ventilated extruder head capture hood that supplied

cooling air in only one direction and captured emissions in a high efficiency particulate air (HEPA) filter through an exhaust port (1.6 L/s). In a test chamber study with one printer, the number of UFPs measured using an SMPS was reported by Dunn et al. (2020) to be reduced by 98.0% and within a simulated MakerSpace equipped with 20 printers each fitted with an extruder head capture hood, the number of UFPs was reduced to below background levels. Viitanen et al. (2021) investigated the effectiveness of a retrofitted LEV system that consisted of a HEPA filter and a canopy hood (capture velocity of 30 L/s, ACH = 3.6) positioned above a ME-type FFF 3-D printer. Compared to room levels with GEV (2.9 ACH) in operation, this system only reduced UFPs by 30% on a particle number basis (SMPS data) and 49% on a particle surface area basis (diffusion charger (DC) data). The distance of the canopy hood relative to the 3-D printer nozzle (minimum 12 cm to 15 cm away) contributed to the low effectivity achieved. The warm extruder nozzle also created an emission plume that rose and might have fluctuated, and was, therefore, not captured by the hood.

Gu et al. (2019) measured particle and VOC concentrations during operation of an FFF 3-D printer (side walls but open top) with an air purifier placed 50 cm from the printer inside a test chamber (30 m^3). The air purifier was used as a ventilation control with either a combination HEPA-activated carbon filter (ACF) or a combination HEPA-high-efficiency multi-oxidation pottery and porcelain granule (HIMOP) filter at medium (approximately 170 m^3/hr) and high (approximately 300 m^3/hr) flow rates. Based upon FMPS measurements, the air purifier reduced the number of UFPs (compared with the scenario of no air purifier) by 74% (HEPA-HIMOP, medium flow rate) to 90% (HEPA-HIMOP, maximum flow rate) and the surface area concentrations (calculated from size data) were reduced by 79% (HEPA-HIMOP filter, medium flow rate) to 92% (HEPA-HIMOP, maximum flow rate). Filters used in the air purifiers showed varying effectiveness in removing VOCs. Total VOCs [calculated as Σ(VOCs)] were decreased by 69% to 71% when the air purifier was equipped with the HEPA-ACF but increased when the air purifier was equipped with the HEPA-HIMOP filter (up to −736%). The ACF-HEPA removed 100% of ethylbenzene and 70% of styrene, while use of the HEPA-HIMOP filter led to elevated concentrations of ethylbenzene (up to −33%) and styrene (up to −200%) (Gu et al. 2019).

Zontek, Scotto, and Hollenbeck (2021) assessed the effectiveness of LEV in a university fabrication lab room with an open floor plan design in which 8 ME-type (FFF) printers were housed. The unspecified make and model printers were open in the front and PLA filament was used while all eight printers operated simultaneously. The LEV system consisted of four inlet openings and ducts positioned in between, but not directly above the printers that had a design velocity of 15.24 m/s (3000 fpm). The LEV reduced particle number concentrations measured using a CNC (0.01 μm to >1 μm) by 13.6% and particle mass concentration (0.3 μm to 10 μm) by 42.3% (Zontek, Scotto, and Hollenbeck 2021).

Secondo et al. (2020) examined ME-type FFF 3-D printer UFP emissions using an SMPS and OPS at three university MakerSpaces: a library MakerSpace (≤4 printers) with typical office GEV (3.1 ACH), a lab MakerSpace with 29 printers inside cabinets that had openings to permit airflow and lab room-type GEV (8.7 ACH), and a center MakerSpace (≤4 printers) with almost no GEV (0.2 ACH). The number of particles rose in the Center MakerSpace

and the GEV exhibited almost no efficacy in reducing the number of particles when using one or up to four printers (−411.0 to −4826.1%, respectively). The investigators tested a portable ACF-HEPA system that was positioned approximately 27 cm from the Upbox+ (using ABS) exhaust (not directly connected to the printer), while it and three Replicator 5th generation printers (using PLA) were operated simultaneously. During this test with the ACF-HEPA system, particle concentration in the Center MakerSpace increased relative to background, which suggested the ventilation was ineffective (−1752.5%). The exact reason why particle number concentration increased while the ACF-HEPA system was in use is not known but could be from fluctuations in background particle concentration (Secondo et al. 2020). Although particle number concentration in the Center MakerSpace increased during the test with the ACF-HEPA system, levels were still lower compared with a test when the same printers were operated with the ventilation system off. In the library MakerSpace, office GEV was not efficient in lowering particle emissions during printing with PLA filament (−1.1 to −627.9%, depending upon the printer), with the exception of the Lulzbot TAZ 5 printer, where particle emission was reduced by 59.1%. Similarly, office GEV was not sufficient in reducing particle emissions during printing with ABS filament. However, Secondo et al. (2020) noted that in the library MakerSpace there were other particle emission sources influencing the background particle concentration and resultant efficacy calculation. In a lab room MakerSpace, the simultaneous use of 29 printers inside enclosures, but with the enclosure doors kept open, and room GEV of 8.7 ACH led to an increase in particle number concentration (−64.9%). Furthermore, Viitanen et al. (2021) stated that with regular or long-term use of ME-type FFF desktop 3-D printers, GEV (2.9 ACH), was not sufficient to control particles <50 nm (measured using an SMPS) in size. Collectively, these studies indicated that, under the specific room conditions evaluated, GEV was inefficient as an engineering control for particle emissions from ME-type FFF 3-D printers. Note that GEV is not considered to be as satisfactory for contaminant control for health protection as LEV because some AM process emissions can possess appreciable toxicity.

Isolation—No reports of isolation controls for BJ or DED machines were identified in the literature search. Eighteen citations reported one or more isolation controls for MJ, VP, PBF, and ME processes.

For the MJ process category, particle levels in a workroom decreased from 76.1% to 93.5% (CNC data) and from 90.0% to 92.3% (OPS data) when a machine was operated with its cover closed (non-airtight) compared with when it was operated with its cover open. In contrast, when the MJ printer cover was closed, TVOC levels rose in the work room (effectiveness of −60.7%) or decreased by just 10.7% compared with when the cover was in the open position (Stefaniak et al. 2019a).

For VP machines, two articles evaluated the efficacy of isolation controls (Han, Zhao, and Li 2021; Yang and Li 2018). Han, Zhao, and Li (2021) described a manufacturing paradigm termed 4-D printing, whereby an AM machine was used to create a 3-D object that possessed stimuli-responsive properties (e.g., shape changes) over time. In this study, a fully enclosed VP printer (non-airtight) was retrofit to include activated carbon adsorbent beds that were positioned inside the printer build chamber. When the VP printer was operated

with activated carbon adsorbent beds, TVOC levels were reduced by 58.9% compared to printing without the beds (Han, Zhao, and Li 2021). Yang and Li (2018) evaluated the efficacy of activated carbon adsorbent as well as a titanium dioxide (TiO_2) photocatalytic oxidation (PCO) method to control TVOC emissions from a VP printer that had a fully enclosed design with a hinged non-airtight cover. For the PCO method, TiO_2 was used as a catalyst to oxidize gaseous organic compounds and for the activated carbon approach, gaseous compounds were adsorbed to the carbon material. Details of the experimental setup were not clear, though it was deduced that the PCO or activated carbon material was placed inside the printer build chamber. During printing, TVOC concentrations were −4.6% (increased), 53.8% (reduced), and 72.2% (reduced) for the enclosure, enclosure with PCO material, and enclosure with activated carbon adsorbent, respectively. The printed parts were subjected to post-processing by rinsing in ethanol and further curing. Details of how these tasks were performed were not provided, but it was reported that TVOC concentration was elevated (−21% effectiveness) for the enclosure only, increased (−4.8% effectiveness) for the enclosure with PCO material, and reduced by 63% when using the enclosure with activated carbon adsorbent. Overall, considering both the printing and post-processing steps, TVOC concentrations were enhanced (−6.1% effectiveness), lowered by 44%, and reduced by 71% for the enclosure, enclosure with PCO material, and enclosure with activated carbon adsorbent, respectively. Based upon total emissions associated with the AM process (expressed as mass in units of μg), activated carbon had the highest efficacy (69% decrease), followed by the PCO material (63% reduction) and the machine enclosure (−17%).

PBF machines are designed with an enclosed and sealed build chamber, and when using metallic powder feedstock, this build chamber is kept under vacuum or purged with nitrogen or argon gas or uses local inert gas shielding (and the AM machine is bonded and grounded) to prevent oxidation and fire (Chen et al. 2020; Stefaniak, Du Preez, and Du Plessis 2021a). Azzougagh et al. (2021) simultaneously monitored particle concentrations inside the sealed and enclosed build chamber of a PBF machine via a port and in a workroom using a CNC; during printing with metallic powder, this machine enclosure reduced particle concentration in the workroom by up to 90.0%.

ME-type FFF 3-D printers with manufacturers' designed isolation control were evaluated in five articles. Enclosures (usually non-airtight) designed for many early model FFF 3-D printers were likely intended to maintain thermal stability in the build chamber to prevent part warping, rather than contaminant control. Yi et al. (2016) tested an FFF 3-D printer with sidewalls and a plastic cover provided by the manufacturer that rested on the top of the machine to form a full non-airtight enclosure; reduction of particle number levels ranged from 45% (OPS data) to 68% (electrical low-pressure impactor (ELPI) data) in a test chamber and 74% (SMPS data) in an office room. In a follow-on study using the same printer and chamber setup, Stefaniak et al. (2017b) reported that the loose-fitting cover increased overall background-corrected TVOC emissions (effectiveness of −3.6%) in a test chamber, though background-corrected concentrations of some individual VOCs were reduced: isopropyl alcohol (70%), ethylbenzene (76%), and styrene (37%). Azimi et al. (2016) found that for the same model printer as used in the Yi et al. (2016) and Stefaniak et al. (2017b) studies, the loose-fitting cover reduced particle number in a test chamber by 35% (CNC data) relative to printing without the cover, and affirmed that when the cover was

in place, it was largely ineffective in lowering concentrations of VOCs (Azimi et al. 2016). Du Preez et al. (2018) observed that for one model of fully enclosed FFF 3-D printer (side walls and non-airtight cover), particle number concentrations measured using a CNC in an office were reduced by 6–90% (compared to with the cover off), which varied with filament type and color. Zontek et al. (2017) demonstrated that a fully enclosed FFF 3-D printer with a hinged front door (non-airtight), based on SMPS measurements inside and outside the enclosure, reduced UFP concentration in a room by 94.7% on a number basis and 99.9% on a mass basis (calculated from SMPS size data).

ME-type FFF 3-D printers with retrofit isolation controls were examined and efficacy noted in eight studies. Wilkins, Traum, and Wilkins-Earley (2020), as part of a school learning curriculum, stacked two plastic tables one atop the other and attached poly(methylmethacrylate) (PMMA) panels on all four sides to create an enclosure. An FFF 3-D printer was placed on the surface of the bottom table and under the top table. During operation of the FFF 3-D printer inside this enclosure, particulate matter (PM) with aerodynamic diameter less than 10 μm (PM_{10}) was monitored using an OPS. Compared with the scenario of an unenclosed printer, PM_{10} levels in the classroom increased when operating the printer inside the enclosure for PLA (−77.1% effectiveness) and polyethylene terephthalate-glycol modified (PETG) (−53.4% effectiveness) filaments but were decreased by 24.3% for ABS; similar trends were noted for PM with aerodynamic diameter less than 2.5 μm ($PM_{2.5}$) levels.

Several investigators designed their own isolation controls from commercially available parts and evaluated performance. Wojtyła, Śpiewak, and Baran (2020) assessed the efficacy of graphitic carbon nitride as a PCO approach to degrade VOCs emitted from an FFF 3-D printer using a high impact polystyrene filament. To improve photocatalytic activity, graphitic carbon nitride was doped with iron, bismuth, manganese, or antimony. Each doped photocatalytic material was placed inside a test chamber with the printer; compared to the scenario of non-photocatalytic material, use of antimony-doped graphitic carbon nitride performed best, with observed reductions in styrene, ethylbenzene, and cumene emissions of 87%, 73%, and 86%, respectively. In a study of emissions during compounding to make nano-filled polymer and FFF 3-D printing with the polymer, for all tasks conducted in a retrofit half-enclosure, the average particle surface area and number concentration in workplace air measured using a diffusion charger were increased (compared to printing without the enclosure) as documented by −34.7% and −100.9% effectiveness, respectively (Oberbek et al. 2019). In another study involving nanofillers, emissions were evaluated for an open-frame prototype hybrid FFF 3-D printer/plasma jetting machine that was isolated inside a PMMA box (López De Ipiña et al. 2021). The box had an LEV system, though it was turned off during testing. For FFF 3-D printing with the base polymer and nano-filled polymers, the unventilated box had limited efficacy to contain particles on a number basis (inside box compared with room air), i.e., −11.3% (increase in the room) to 48.2% decrease (CNC data) and −18.4% (increase in the room) to 82.1% decrease (OPS data). Microscopy samples of particles released by the machine did not identify any free or polymer-bound nanofillers (López De Ipiña et al. 2021). Viitanen et al. (2021) reported that an unventilated plastic enclosure (material not specified) that was placed over an FFF 3-D printer with a back wall but no side walls or top reduced particle levels by 97% (SMPS data) and 89%

(DC data) for number and surface area, respectively, compared to no enclosure with 2.9 ACH of GEV in the room. As shown in Table 1, the efficacy of this enclosure was higher compared with a retrofit LEV canopy hood placed over the same model printer (30% and 49%, by number and surface area, respectively). Cao et al. (2019) placed a custom-made poly-acrylonitrile nanofiber filter in a PMMA box that housed an open frame FFF 3-D printer. Using a haze detector, it was determined that during 3-D printing, the filter material reduced $PM_{2.5}$ concentration by 81% compared with outside the box (Cao et al. 2019).

The previously described studies of retrofit enclosures were for a single ME-type FFF 3-D printer. Data on efficacy of isolation as a control for multiple FFF 3-D printers operating simultaneously are scarce. Runstrom Eden et al. (2022) evaluated emissions from three ME-type FFF 3-D printers (two had side walls but no top or front and one had side walls and split front doors but no top) placed in a hood enclosure (no other details given); during printing with various filaments, particle number concentration (CNC data) was 98% lower in the workroom compared with inside the enclosure. In a study with 29 FFF 3-D printers in a lab room MakerSpace (n = 27 with side walls and no top and n = 2 with side walls but no top or front) that were housed in 5 unventilated cabinets with non-airtight doors, Secondo et al. (2020) found that particle number concentration (SMPS and OPS data) in the room increased during printing with PLA filament, i.e., effectiveness was −9.8 to −70.1%.

For large format AM machines, a type of ME process that involves extruding kilogram quantities of feedstock per hr, investigators examined loose-fitting custom-built canopies placed over two different models of machines to enclose the build chambers while printing with several different polymers (Stefaniak et al. 2021c). Among all polymers tested, the canopies were ineffective; on average, particle concentrations in the room measured using a CNC were elevated compared with inside the enclosure (−27.4% effectiveness) with range −313.6% (increased) to 77.8% (decreased) and average TVOC concentrations in the room were −281% (elevated) with range −925% (increased) to 58.8% (reduced).

Ventilated enclosures—Publications from several research groups mentioned reductions in emissions by ventilated enclosures for MJ, VP, PBF, and/or DED processes (Ding and Ng 2021; Hayes et al. 2021; Runstrom Eden et al. 2022); however, there were insufficient data in these reports to calculate efficacy. Twelve articles provided data that met the inclusion criteria for this review (Table 1). One paper evaluated a ventilated enclosure for a DED process, and 11 articles assessed ventilated enclosures for ME-type FFF 3-D printers.

Among investigations that mentioned decreases in emissions but efficacy was not quantified, particle number concentration in workrooms with MJ printers was noted to not change for different models of machines that were designed with sealed and ventilated enclosures, which suggested full containment (Ding and Ng 2021; Runstrom Eden et al. 2022). For a desktop-scale VP printer designed with a hinged cover that closed to form a ventilated enclosure, Runstrom Eden et al. (2022) demonstrated that there was no change in particle number (20 to 1000 nm measured using a CNC) concentration compared with background in a workroom during printing; however, TVOC levels in the room were found to have increased more than twofold above background during printing. For an industrial-scale VP printer designed with a ventilated build chamber, Hayes et al. (2021) noted that there was no

change in particle (11.5–365 nm measured using an SMPS and 0.52–20 μm measuring an aerodynamic particle sizer (APS)) or TVOC levels during printing (Hayes et al. 2021). Ding and Ng (2021) noted that there was no change in the number concentration of UFP and submicron size particles above background in workrooms during operation of a PBF machine (sealed enclosure with recirculating filtration) using metallic feedstock or a PBF machine (sealed enclosure with LEV) employing polymer powder feedstock, which indicated complete isolation of the processes. When doors of the PBF machines were opened, it was found that there was no alteration in particle number concentration above background levels in the workroom (Ding and Ng 2021). With regard to gas-phase emissions, TVOC concentrations in a workroom were detected to have remained similar to background or elevated more than twofold during operation of a fully sealed and ventilated PBF machine while printing with polyamide polymer feedstock (Runstrom Eden et al. 2022).

Oddone et al. (2021) measured the inhalable fraction of several metals inside of a 64 m^3 ventilated enclosure (material not specified) that was retrofit to surround a robotic arm DED process and outside the enclosure at the machine operator's desk. Comparison of metal concentrations inside the enclosure to at the operator's desk indicated that the efficacy of the enclosure ranged from 16.7% (iron) to 70.8% (cobalt). Furthermore, Ding and Ng (2021) found that there was no marked change in particle number concentration above background in a workroom during operation of a DED machine (sealed machine with LEV) using metallic feedstock, which suggested complete isolation, though efficacy could not be quantified from the reported data.

Five articles reported on the efficacy of ventilated enclosures incorporated into ME-type AM machine designs. The same model of fully enclosed FFF 3-D printer with internal recirculating HEPA and ACFs was examined in two different studies using a CNC; efficacy in reducing particle levels ranged from 42% (Du Preez et al. 2018) to 79% (Stefaniak et al. 2019b). A different model of a fully enclosed FFF 3-D printer with an internal recirculating HEPA filter lowered average particle number levels in an office by 94.7% (SMPS data) and average particle mass levels by 91% (aerosol mass spectrometer data) compared with the scenario when air was not circulated through the HEPA filter (Katz et al. 2020). Davis et al. (2019) reported that, contrary to expectation, an FFF 3-D printer designed with a full enclosure and internal recirculating HEPA filter increased TVOC concentration in a test chamber study (−18% effectiveness) compared with the scenario of printing without the filter in place. Additionally, release rates were elevated for styrene, dodecane, decane, tetradecane, xylenes, and benzaldehyde, although % changes in their levels were not provided. Cao and Pui (2020) employed an SMPS to monitor particle number concentration and calculate particle surface area as metrics of containment for a ME-type fused deposition modeling (FDM™) machine with sealed design and internal recirculating HEPA filter; based upon measurements inside and outside the machine enclosure, particle surface area and number concentration were reduced by approximately 100%. Ding and Ng (2021) found that assessment of an FDM™ machine with a sealed enclosure revealed there was no significant change in particle concentration in a workroom during operation, which indicated complete containment; however, data were not provided to permit quantification of efficacy. The sealed build chambers of FDM™ machines might fully contain particles during operation;

however, Du Preez et al. (2018) found that when doors to FDM™ machines were opened after printing, TVOC levels rose above background to nearly 18 mg/m^3, which indicated an acute gas-phase exposure risk for the post-printing task of retrieving built objects.

Several investigators evaluated ventilated enclosures that were retrofit to ME-type FFF 3-D printers, and one article evaluated a retrofit-ventilated enclosure for a plasma-jetting post-printing task. In the study by Wilkins, Traum, and Wilkins-Earley (2020), when a suction fan was used to provide LEV to the enclosure made from stacked tables and PMMA panels, PM_{10} mass levels measured using an OPS in the classroom were either slightly decreased (ABS filament) or similar (PLA and PETG filaments) compared with the unventilated enclosure. Viitanen et al. (2021) noted that when a plastic enclosure (material not specified) that was placed over an FFF 3-D printer (back wall, but no side walls or top) was ventilated, particle reductions were 99% and 96%, for particle number (SMPS) and surface area (calculated from SMPS size data), respectively (compared with 97% and 89% for number and surface area, respectively, in the unventilated enclosure with room ACH of 2.9). Both the ventilated and unventilated enclosures performed better than a canopy hood with HEPA filtration positioned over the printer (30% and 49% for number and surface area, respectively) (Viitanen et al. 2021). Investigators at the Health and Safety Executive (HSE 2019) placed a PMMA a box over an open frame FFF 3-D printer. The box was fitted with an exhaust fan and HEPA filter with activated carbon coating on the inner surface. This isolation control was tested in two modes “exhausting” where spacers were placed under the box to create a gap that allowed air to be pulled from the base of the box past the printer to the fan and HEPA-ACF on the top of the box and exhausted into the room and “recirculating” where the box rested on a surface to form a seal and air was recirculated through the HEPA-ACF inside the box. The reduction in particle number concentration in a room (relative to printing without the box), as determined using a DC, was 97% (exhausting) to 99.4% (recirculating) (HSE 2019). In a study of multiple retrofit control options, Kwon et al. (2017) placed an FFF 3-D printer (side walls only) in a box (unspecified material) and determined the efficacy of the box with LEV and the box with LEV coupled to various filters to reduce particle number concentration (monitored using an SMPS). For the enclosure with LEV, compared to printing with no enclosure, background-corrected particle number concentration was lowered by 74.4%. When the enclosure with LEV (suction nozzle) was modified to include an ACF that was positioned at the extruder nozzle, compared to printing with no enclosure, background-corrected particle number concentration was decreased by 90.7%. Finally, Kwon et al. (2017) evaluated the enclosure with LEV and various filters; compared to printing with no enclosure, background-corrected efficacy ranged from 76% (combination electret/antibacterial filter) to 99.95% (HEPA filter). One study (Stefaniak et al. 2019b) reported the efficacy of an enclosure for multiple printers. Stefaniak et al. (2019b) attached PMMA panels around shelving that housed 10 FFF 3-D printers (all with side walls and non-airtight covers) to form a non-airtight enclosure and ventilated it using a fan with HEPA filter and ACF; particle number (SMPS and CNC data) and TVOC concentrations in the room (no ventilation) were decreased by 99.7% and 53.2%, respectively.

Among published papers that evaluated ventilated enclosures that were retrofit to ME-type FFF 3-D printers, only Gu et al. (2019) assessed a control that was specifically designed

by an FFF 3-D printer manufacturer for its brand of machines. Gu et al. (2019) measured particle and VOC concentrations during operation of an FFF 3-D printer (side walls but open top) with an after-market filter cover designed to seal the machine and form a full enclosure; the cover had an exhaust fan and HEPA-ACF unit. This after-market design lowered both particle number (FMPS data) and surface area (calculated from FMPS size data) concentrations in a test chamber by 93 (compared to printing without the cover). The efficacy of this after-market cover to contain particles was similar or slightly better compared with the same printer retrofit to position air purifiers with various filters near the machine (Table 1). The efficacy of the after-market filter cover for gas-phase emissions was inconsistent. The concentration of ethylbenzene was reduced by 100% and styrene was decreased by 15% but TVOCs (calculated as the sum of individual VOCs) was increased (−16% effectiveness) in the test chamber (Gu et al. 2019). Interestingly, new VOCs were detected during the use of the filter covers that were not present when printing without the control in place. Specifically, use of the filter cover released isopentane, dichloromethane, tetradecane, hexadecane, octadecane, and other iso/cycloalkanes.

Much attention has been given to isolation controls for the printing step in ME-type FFF 3-D printing processes; however, exposures might also occur during pre-printing, post-printing, and post-processing tasks. López De Ipiña et al. (2021) reported that a prototype hybrid FFF 3-D printer/plasma jetting machine housed in a PMMA box enclosure with LEV was used to print bone scaffolds and then surfaces were plasma treated. During the plasma jetting post-printing task, particle number concentrations in a lab room were reduced by greater than 97% (CNC data) and up to 95.7% (OPS data) (López De Ipiña et al. 2021).

Administrative controls

Administrative controls occupy the fifth tier in our version of the hierarchy of controls (Figure 1). Of the published papers related to administrative controls, three provided information on controls related to area/workplace specifications, three focused on the influence of print parameters, and seven reported information aimed at evaluating the printer setup/criteria.

Area/workplace specifications—Three studies monitored concentrations in the near field (NF) and far field (FF) in areas/workplaces adjacent to an AM process, to assess the influence of different sampling distances on contaminant concentrations. Zhou et al. (2015) demonstrated that particle number concentrations were elevated from near an open frame FFF 3-D printer (NF) compared with 1.8 m from the printer (FF), i.e., −50% effectiveness, and rose from near the printer compared with 4 m from the printer (FF), i.e., −83% effectiveness. The particle number concentration increased even higher from near two open-frame FFF 3-D printers (NF) compared with 1.8 m from the printers (FF), i.e., −419% effectiveness. This study was carried out in a clean room using an OPS instrument to measure number concentration while printing with different color ABS feedstocks. Based upon these data, Zhou et al. (2015) concluded that particle concentrations were higher as distance increased from the printer. In another study, Lewinski, Secondo, and Ferri (2019) demonstrated that stationary particle measurement results presented as background-corrected total particle mass (gravimetric analysis of filter samples) were 0

to 0.08 mg/m^3 within 1 m (NF) of a BJ machine and 0.02 mg/m^3 at a distance of 3 m (FF) from the machine when stainless steel powder feedstock was used for a 75% reduction in mass concentration with distance. Stefaniak et al. (2022) monitored particle number (APS, OPS, and CNC data) and TVOC releases in the NF and FF during (1) granulation of waste ABS and PLA plastics, (2) extrusion of granulated waste materials into filament, (3) extrusion of virgin polymer pellets into filament, and (4) FFF 3-D printing with recycled and virgin plastic filaments. The effect of distance was highly variable, with some background-corrected particle number and TVOC concentrations rising with distance and others decreasing with distance; most particle number and TVOC concentrations were not markedly different between NF and FF locations (Stefaniak et al. 2022).

Print parameters—Three studies specifically aimed at identifying the influence of ME-type FFF 3-D printer manufacturing parameters as possible control measures to reduce particle emissions. Deng et al. (2016) investigated both ABS and PLA filaments along with two print parameter combinations (nozzle temperature and filament feed rate). Nozzle temperatures and feed rates were changed according to the baseline settings specific to each filament material. The influence of printing with different nozzle temperatures indicated that particle emissions from PLA printing were orders of magnitude lower than ABS printing. The different filament feed rates displayed less of an effect on particle emissions. Deng et al. (2016) noted that the main contributor to particle emissions was pre-heating the extruder nozzle with filament present. From their emissions monitoring using a CNC, it was recommended to preheat the extruder nozzle and build a platform before ABS filament is loaded into the nozzle to reduce particle number by up to 75% (Deng et al. 2016). Simon et al. (2018) reported that increasing the print speed from 25% of the default setting to 150% of the default setting increased UFP number concentration as measured using an SMPS (−280% effectiveness) in a clean room. The authors observed that if the filament was retracted from the extruder nozzle during the nozzle heating step, there was still a spike in UFP number concentration (up to 475,000 #/cm^3). This observation indicated that filament residue in the extruder nozzle might contribute to emissions. When the extruder nozzle was cleaned, the peak UFP number concentration was reduced to 150 #/cm^3, which indicated a 100% reduction compared with the nozzle that contained filament residue. The authors concluded that during pre-heating of the extruder nozzle, if the filament is “wet” (dripping in the nozzle during heating) it can emit semi-volatile organic compounds, which may condense, and form particles in air. In addition, even if the filament is retracted from the extruder nozzle during heating, there might be filament residue in the nozzle from prior printing, which initiates a spike in particle emissions when the printing step commences. Finally, Simon et al. (2018) demonstrated that changing the material flow and distance between the extruder nozzle and build platform did not markedly affect particle emissions. Khaki et al. (2021) also observed that particle emissions increased rapidly during extruder nozzle pre-heating. Cheng et al. (2018) experimented with different infill settings (heights, densities, patterns) and filament feed rate during printing of the first top layer to determine their influence on peak particle emissions. The infill of an object refers to the inner portion of the object that is surrounded by the outer shell. Infill density ranged from 0% to 100%. Infill patterns include linear (i.e., grid pattern), honeycomb (i.e., hexagonal pattern), and others. Particles were monitored using an OPS (0.3 to 2.5 μm) during all printing tests.

Filament feed rate reduction was only investigated for the first top layer printing while for other printer layers the feed rate was held constant. Based upon their experiments, Cheng et al. (2018) concluded that optimal settings were less infill height, higher infill density, and printing at a slower feed rate (at least for the first top part), which resulted in a 96% decrease (compared with the peak level from each tested setting) in particle emissions. In support of this observation, Khaki et al. (2021) also noted that with increasing infill density, PM with size <0.3 μm emission levels (OPS data) fell.

Printer setup/criteria—The printer setup/criteria describe administrative controls related to user-adjustable AM process settings. Two studies applied warning sensors as administrative controls while investigating ME-type FFF 3-D printer emissions. Wojnowski et al. (2020) examined a 3-D printer in an enclosure while printing with different ABS filaments and monitored changes in benzene, toluene, ethylbenzene, xylenes (BTEX), and styrene concentrations. Concentration changes inside the enclosure were monitored in parallel using realtime Proton Transfer Reaction Mass Spectrometry and a prototype electronic “nose” fitted with seven electrochemical sensors. Data indicated that the threshold limit value for the concentration of BTEX exceeded the 0.96 classification accuracy within a 5-min time-frame based upon the reaction time of the chemical sensors. In another study, $PM_{2.5}$ emissions were monitored using an OPS in an indoor home setting while printing with ABS and PLA filaments (Khaki et al. 2021). Simultaneously, $PM_{2.5}$ emissions were monitored before, during and after printing with a low-cost indoor air quality sensor (Cair sensor, NuWave, Ireland). Both instruments were placed 1 m from the printer nozzle. The impact of different print parameters such as print speed, filament diameter, bed temperature, filament color, fan speed, infill density, and extruder temperature were also investigated. For comparison between the OPS and Cair sensor, Khaki et al. (2021) presented sensor responses instead of sensor behavior data to highlight precision over a range of print conditions. Both sensors indicated consistent $PM_{2.5}$ profiles with similar onset times in $PM_{2.5}$ elevations for each print. The maximum $PM_{2.5}$ emission for both sensors was similar in magnitude for most emission profiles; however, following the maximum $PM_{2.5}$ emission, the decay profiles differed between sensors for certain prints. Khaki et al. (2021) concluded that both sensors exhibited the ability to indicate at what time point a significant rise in $PM_{2.5}$ occurs, thereby enabling a user to become aware of the influence of specific print parameters on indoor air quality and take corrective actions.

Four studies reported on the time delay required to reduce emissions concentrations inside enclosures to background levels prior to retrieving printed objects from various types of AM machines. The earliest investigation was from Zhou et al. (2015) who conducted two experimental setups, both with ME-type FFF 3-D printers in fixed positions while determining the distribution of fine particles in three different locations. Zhou et al. (2015) operated the ventilation system prior to printing for removal of background contaminants from the clean room. Thereafter, the ventilation system (90 ACH) was switched off during printing and switched on again after printing for removal of any particles from printers. Data showed a significant decline in particle concentrations that took 10 min for particles to reach background levels for one printer and 40 min to reach background for two printers (Zhou et al. 2015). As noted in the section on Isolation controls, investigators at the HSE

(2019) placed a PMMA box over an open frame FFF 3-D printer and measured the control in “exhausting” mode and “recirculating” mode; for both modes, it took 20 min for particle concentrations inside the PMMA box to return to background levels. Stefaniak et al. (2019b) assessed emissions at a facility with 10 freestanding desktop FFF 3-D printers on shelving in a room that did not have LEV or general exhaust ventilation. These investigators built a custom-designed ventilation enclosure that consisted of hinged PMMA panels attached to the shelves. The enclosure was ventilated with a portable floor fan attached to HEPA and activated carbon filters in series. Particle number concentrations were measured with a CNC and TVOCs inside the enclosure; within 30 min, particle number concentration decreased 98.4% (to near background) and TVOC concentration fell 69.5% (Stefaniak et al. 2019b). Bau et al. (2020) determined particle emissions during a DED process for two powder materials (Stainless steel 316 L and Inconel 625) and two injection nozzle settings. The DED machine had a sealed and ventilated enclosure. For a transient door opening step, particle number concentration was measured inside the machine and in the NF to approximate the operators normal work location. The transient door opening step resulted in peak particle number concentrations that exceeded 10^5 #/cm^3 in the NF. To address this exposure risk, two additional machining cycles were run but after the completion of each cycle, the machine door was kept closed with a time delay of 8 min, which lowered concentration inside the ventilated enclosure by a factor of 10 (but not as low as background) and eliminated the peak exposure risk, as documented using a particle counter that was positioned in the operator’s breathing zone. Bau et al. (2020) concluded that a time delay before allowing the machine doors to be opened would reduce operator exposure during this task.

Han, Zhao, and Li (2021) measured the effectiveness of several administrative controls to lower organic gas emissions during a 4-D printing process, which involved printing with a commercial desktop VP-type laser stereolithography printer in a lab room followed by tasks to induce shape changes in the printed object. During a material preparation pre-printing task, two different stirring speeds were applied to mix ingredients; reducing the stirring speed from 500 rpm to 250 rpm lowered TVOC concentrations by 9.5% (Han, Zhao, and Li 2021). The final two stages were post-processing tasks that involved shape programming and shape recovery. During shape programing, use of a water bath instead of a hot plate decreased TVOC levels by 88% and lowering the water bath temperature from 62°C to 52°C reduced TVOC levels by 39%. Similarly, for shape recovery, lowering the water bath temperature from 62°C to 52°C reduced TVOC levels by 39% (Han, Zhao, and Li 2021).

Personal protective equipment—The last tier in our version of the hierarchy of controls is the PPE category (Figure 1). Graff et al. (2017) investigated a PBF process using Inconel 939 powder feedstock that included (1) powder characterization, (2) static area monitoring of the workplace environment (including emissions and metal concentrations in the workplace area), and (3) personal exposure monitoring of AM operators (including task-based monitoring). The results from the AM operator’s personal exposure to inhalable metals confirmed the presence of chromium (44 μg/m^3), nickel (99 μg/m^3), and cobalt (38 μg/m^3). As most AM tasks are performed manually by the AM operator, different tasks were monitored to determine the airborne metal particle emissions in the range of 0.3 to

10 μm; peak number concentration in the 0.3 μm size fraction during machine opening, sieving, and vacuuming and cleaning ranged from 5.0×10^7 #/m^3 to more than 1×10^8 #/m^3. AM operators were provided with powered air purifying respirators (Sundström SR 500, TH3, protection factor 250, fitted with an integrated P3 filter and prefilter). The respirator was designed for the protection against hazardous particles, vapors, and gases and was equipped with two SR 510 P3 particle filters (99.95% removal rating) with a SR 221 particle prefilter. Graff et al. (2017) investigated the efficacy of the PPE by performing OPS measurements (0.3 to 10 μm) inside and outside the respirator. Outside, particle mass peaked at approximately 150,000 μg/m^3 while inside almost no particle mass was detected, which confirmed that the PPE removed greater than 99% of particles and complied with their safety criteria. The facility also implemented protective clothing for AM operators, designed for nanoscale particle exposure.

Descriptive summary of available emissions data

Particles—A crude summary of all 148 particle control efficacy values in Table 1 revealed median efficacy values of 99% (PPE), 72.0% (administrative), 47.2% (engineering), and −4.2% (substitution) for these tiers of the hierarchy of controls (Figure 2). Note that the PPE tier has only one efficacy data point, and thus is not a true median. For the remaining tiers, medians were based upon all AM process types and all particle data, regardless of measurement strategy (e.g., type and positioning of instruments) or metric (i.e., number, mass, or surface area).

As illustrated in Figure 3, for FFF 3-D printers only, from the 94 available number-based efficacy values (all instruments), the median efficacy values for control of particles were 68.9% (administrative), 60.0% (engineering), and −4.2% (substitution). There were no data available on the efficacy of PPE for FFF 3-D printers

Approximately 69% (65/94) of available efficacy values for FFF 3-D printers were for the engineering tier of the hierarchy of controls (there were only 11 efficacy values for administrative controls and 18 for substitution controls, and hence these tiers were not evaluated further because of small sample numbers). As presented in Figure 4a, based upon calculated medians, the efficacy of engineering controls by type for particle number-based measures of emissions from FFF 3-D printers were (n = 65 values) as follows: ventilated enclosures (95.0%), ventilation (80.9%), and isolation (41.4%). Note that because GEV data were excluded from these analyses, for FFF 3-D printers, the ventilation grouping is equivalent to LEV. After excluding the three values reported as combined OPS/SMPS data in a published paper, the remaining 62 efficacy values were further stratified into two size fractions: fine particles (OPS, CNC, and diffusion charger data) and UFP (ELPI, FMPS, and SMPS data). From Figure 4c, median efficacy values by engineering control type for fine particles emitted by FFF 3-D printers were (n = 38 values) as follows: ventilated enclosures (88%), ventilation (13.6%), and isolation (37.1%). As given in Figure 4d, median efficacy values for UFP emitted by FFF 3-D printers were (n = 24 values) as follows: ventilated enclosures (95%), ventilation (88%), and isolation (84%). These data indicate a potential particle-size dependent effect in the efficacy of engineering controls for FFF 3-D printers.

The 65 particle number-based efficacy values for engineering controls were further stratified by implementation (i.e., retrofit or by design). As shown in Figure 5a, for ventilated enclosures, this type of control exhibited a median efficacy of 97.0% when retrofit to a printer compared with 52.6% when implemented as part of a manufacturer's machine design. For isolation, this type of control displayed a median efficacy of 45.1% when it was part of a manufacturer's machine design compared with 33.4% when it was retrofit. No comparison could be made for ventilation because all available number-based particle data were for retrofit ventilation controls. In addition, the engineering control data were stratified by study setting (i.e., test chamber or real-world). As summarized in Figure 5b, based upon median values, efficacy of all types of engineering controls was similar or higher in test chamber settings compared with real-world settings. Specifically, for ventilated enclosures, the efficacy in test chamber settings was 95% (compared with 89% in real-world settings), for ventilation the efficacy in test chamber settings was 86.8% (compared with 30% in real-world settings), and for isolation, the efficacy in test chamber settings was 52.7% (compared with 37.1% in real-world settings). Further stratification of controls by implementation or study setting and particle size (UFP or fine particles) was not feasible as there were often fewer than three efficacy values available in each grouping to calculate medians.

Gases—From the 68 values on efficacy of controls for gas-phase contaminants in Table 1, the calculated medians were 73.5% (administrative), 53.9% (engineering), and 47.2% (substitution) for these tiers of the hierarchy of controls (Figure 2). Note that the medians were calculated from just three efficacy values for the administrative tier and four for the substitution tier. Furthermore, caution is warranted because these medians were based upon all AM process types regardless of measurement strategy (e.g., positioning of instruments or samplers), metric (i.e., individual VOCs or TVOC), and collection method (evacuated canisters, sorbent tubes, or PIDs).

As summarized in Figure 3, based on 58 efficacy values for just ME-type FFF 3-D printers and MJ printers, the calculated medians were 73.5% (administrative), 55.6% (engineering), and 47.2% (substitution) for these tiers of the hierarchy of controls. An attempt to stratify data between TVOC and individual VOC measurements was undertaken to assess their relative influence on these tiers of the hierarchy; however, except for the engineering tier, all combinations of sample type (individual VOC or TVOC) and hierarchy tier exhibited fewer than five efficacy values to calculate a reliable median, which precluded our ability to gain insights on the influence of these factors on reported control strategies. As illustrated in Figure 4b, within the engineering tier, medians by type of control for gases were 69.4% (ventilation), 34.1% (ventilated enclosures), and 3.6% (isolation). Note that none of the ventilation data were for GEV, thus the ventilation grouping was equivalent to LEV. There were too few data points to permit further stratification of engineering controls by implementation (retrofit versus by design) or study setting (test chamber versus real-world).

For ME-type FFF 3-D printers only, the calculated medians were 73.5% (administrative), 47.2% (substitution), and 23.9% (engineering) for tiers of the hierarchy of controls. Note that medians were calculated based upon only three data points for the administrative tier and four for the substitution tier. Interestingly, for the combined FFF 3-D printer and MJ

data, the median efficacy for the engineering tier was 55.6%, whereas for FFF 3-D printers only, the median efficacy value for the engineering tier was 23.9%. Over 80% (30/37) of efficacy values for ME-type FFF 3-D printers were for the engineering tier. Based upon median, the efficacy of engineering controls by type for gas-phase emissions from FFF 3-D printers were 34.1% (ventilated enclosure), 28.2% (ventilation), and 14.6% (isolation). Note that for the combined FFF 3-D printer and MJ data, the median efficacy for ventilation was 69.4%, whereas for FFF 3-D printers only, the median efficacy value for ventilation was just 28.2%.

For MJ printers, all 21 efficacy values obtained from the literature were for the engineering tier (median of 66.7%) of the hierarchy of controls. Within this tier, there were no apparent data available for ventilated enclosures. For the remaining control types, the median efficacies were 71.4% (ventilation) and −25% (isolation).

Discussion

Our version of the hierarchy of controls contained six tiers (Figure 1). No relevant literature was identified for the second tier, elimination controls (Table 1). In some cases, AM processes are considered superior to traditional manufacturing processes because these construct previously impossible geometries (Ford 2014). Hence, the absence of data for elimination controls might reflect the unique attributes of AM processes relative to traditional formative (e.g., injection molding) and removal (e.g., machining) techniques. For all other tiers in our version of the hierarchy, at least one control solution was identified in the literature.

Knowledge of the efficacy of controls for AM processes is critical for their incorporation into risk assessment frameworks to mitigate health hazards from emissions (Dugheri et al. 2022; Petretta et al. 2019). One study applied a control banding approach to evaluate risk specifically for AM processes that utilized metallic feedstocks (Dugheri et al. 2022). Based upon a severity score (properties related to the exposure material such as carcinogenicity or reproductive toxicity) and a probability score (factors related to work such as the amount of material used), the authors assigned risk levels to various tasks. Recommended controls included use of GEV (risk level 1), use of fume hoods or LEV (risk level 2), use of enclosures (risk level 3), and consultation with a specialist (risk level 4). Petretta et al. (2019) presented a detailed risk assessment that identified exposure to VOCs and particles as relevant hazards for 5 types of AM processes (DED was not considered to be a source of emissions and SL was not included in their risk assessment). For VP and BJ processes, these investigators recommended a combination of engineering controls (enclosures, ventilation, and filtration), administrative controls (access restrictions, exposure monitoring, housekeeping, and training), and PPE (to be selected for the specific process), which reduced exposure risk from their “very high” risk category to their “acceptable” or “medium” risk categories. For MJ, ME, and PBF processes, Petretta et al. (2019) recommended all the same controls, except PPE. As documented in Table 1, the efficacy of some of these control solutions identified by Petretta et al. (2019) including enclosures, GEV, LEV, filtration, and PPE have been evaluated; however, others have not, such as access restrictions and training. It is worth noting that multiple studies demonstrated that, under the

specific room conditions evaluated, GEV was insufficient to control particle emissions from ME-type FFF 3-D printers (Secondo et al. 2020; Viitanen et al. 2021); however, GEV is usually not recommended as the primary approach to control hazardous chemicals. Further, based upon calculated median values from available data for particle emissions from FFF 3-D printers and MJ printers, among types of engineering controls, isolation was generally less effective than ventilation or ventilated enclosures. Hence, it is prudent to verify the efficacy of engineering controls that are implemented for AM processes.

Measurements of UFP exposures in various industries (such as asphalt work, machining, welding, and so on) and the ambient atmosphere are heterogeneous and require harmonization of measurement strategies to improve comparability of data (Kumar et al. 2010; Viitanen et al. 2017). As summarized in Table 1, studies of AM emissions are similarly limited by the lack of standardized measurement approaches. In addition, the use of multiple particle metrics to characterize particle releases from AM processes such as number (UFP), mass ($PM_{2.5}$ or PM_{10}), and surface area reflects the state of existing literature and points to the need for standardization. The use of multiple sampling instruments and particle metrics limited our ability to directly inter-compare published data because there were few values on the efficacy of controls for any given instrument and metric. This limitation was especially evident when attempting to stratify particle efficacy values for engineering controls for FFF 3-D printers by UFP and fine particle size. Median efficacy values indicated a potential size-dependent effect for engineering controls, with better reductions in particle levels for UFP compared with fine particles. Note that there are a few limitations to this finding. Firstly, for purposes of calculating median efficacy values, all CNC data were included in the fine particle size fraction. Depending on the model and working fluid, CNCs can detect particles with size of approximately 10 nm (in the ultrafine range) up to a few micrometers. Since this type of instrument is not size-specific, it was unknown if the CNC values represented UFP, fine particles, or both. Secondly, the finding of different efficacies based upon particle size fraction was in consideration of small numbers of values. Future studies are needed to further evaluate the influence of particle size on the efficacy of engineering controls. In addition, no further stratification to account for particle size and implementation (retrofit compared with by design) or study setting (test chamber compared with real-world) was feasible because of small numbers of data. For more information on measurement approaches used to quantify AM emissions for monitoring and testing of controls, readers are referred to the Supplemental File and recent review articles (Chen et al. 2020; Stefaniak, Du Preez, and Du Plessis 2021a).

Prevention-through-design

MacCuspie et al. (2021) demonstrated that CFD modeling may be used for proactive design of workspaces and validated their modeling approach by monitoring and mapping particle concentrations in a Class 1000 clean room. Data demonstrated that forced clean airflows in a space might lower exposures and that CFD modeling may be used without having to replicate physical experiments to better design workspaces. The results indicated a novel paradigm for the design of AM workspaces and lab rooms that may be used for proactive exposure mitigation.

Available literature indicates that more opportunities might exist for incorporation of PtD concepts into AM processes. Jiang et al. (2021) reported that objects printed on a ME-type FFF 3-D printer using cellulose/PLA filament that was surface modified with 3-aminopropyltriethoxysilane were better able to remove formaldehyde from room air compared with activated carbon. The purpose of that study was to build objects for passive removal of formaldehyde from indoor air; however, PLA feedstock is known to emit formaldehyde during FFF 3-D printing (Stefaniak, Du Preez, and Du Plessis 2021a). As such, this modified filament might be a means to develop feedstock materials that self-reduce or -eliminate formaldehyde emissions during FFF 3-D printing. Potter et al. (2019) noted that the presence of carbon nanotubes in the ABS feedstock lowered TVOC emissions during ME-type FFF 3-D printing, though levels of specific VOCs such as α-methylstyrene and benzaldehyde were increased. Additional research is needed to explore the efficacy and safety of filament modification as a PtD control solution.

Opportunities might also exist to apply PtD concepts to post-printing tasks. One example is retrieval of printed objects. For PBF machines, retrieval requires that the operator brushes away excess powder and manually remove the object. For FDM™-type ME process machines, retrieval involves the operator opening a sealed door to access a printed object (Du Preez et al. 2018). Efforts are underway to design end-to-end automation of printing and post-printing tasks for improved productivity (Lim and Pham 2021). Such automation to improve productivity might also help to reduce or eliminate exposures during high exposure tasks by limiting human-machine interactions. Research is needed to assess the efficacy of automated part retrieval systems to minimize operator exposure for AM processes.

Substitution controls

Preliminary data from two studies indicated that the influence of polymer recycling on emissions was highly variable (Table 1). Numerous reasons might explain this variability, including the (1) source of waste plastics as noted by Väisänen et al. (2021), (2) types of additives used in plastics for food packaging may differ from 3-D-printing-grade plastics, (3) presence of product residues on recycled plastics (Mylläri et al. 2016), and (4) filament making and 3-D printing conditions. In the study by Stefaniak et al. (2021b), relative to virgin filaments, all recycled filaments emitted lower TVOC concentrations. Thermal reprocessing of polymers might lower VOC emissions because the most volatile constituents are released from a polymer during initial extrusion (heating), and progressively less volatile constituents are released with each additional extrusion cycle (Väisänen et al. 2021). Finally, an important aspect of the study by Väisänen et al. (2021) was that after each TC, these investigators also examined the mechanical properties of PLA and PP plastics. Data demonstrated that recycled plastic filaments possessed acceptable mechanical performance that made them a plausible alternative for FFF 3-D printing feedstock. Given the promising outlook for recycled plastic feedstocks for FFF 3-D printing, more research on emissions might aid in assessing the efficacy of these materials as substitution controls.

Engineering controls

Multiple studies evaluated the efficacy of engineering controls to reduce or eliminate emissions from MJ, ME, VP, PBF, and DED processes (Table 1). The majority of available

data for the control of particles were limited to ME-type FFF 3-D printers. Available data for control of gas-phase emissions were mostly for ME-type FFF 3-D printers, and to a lesser extent, MJ printers.

Particles—Under the specific room conditions evaluated in multiple studies, GEV was ineffective in controlling particle emissions from ME-type FFF 3-D printers (Secondo et al. 2020; Viitanen et al. 2021). Based upon the 65-particle number-based efficacy values for FFF 3-D printers, available data indicated that any type of engineering control that included LEV, i.e., ventilated enclosure (95% efficacy) or standalone LEV (81% efficacy) performed better than isolation alone (41% efficacy). This observation indicated that future research on engineering controls for particle emissions for FFF 3-D printers might increase efficacy by inclusion of LEV as part of the strategy. There were little data available to provide guidance on the positioning, distance, and capture velocity of LEV relative to an FFF 3-D printer. Zontek, Scotto, and Hollenbeck (2021) reported that an LEV system that consisted of 4 inlet openings and ducts positioned in between, but not directly above FFF 3-D printers, with a design velocity of 15.24 m/s (3000 fpm) generally exhibited poor efficacy in reducing particle number and mass concentrations. Viitanen et al. (2021) suggested that LEV efficacy might be higher in FFF 3-D printers that are designed with a fixed nozzle position and moveable printing bed, since the LEV hood can be positioned closer to the print nozzle; however, high airflow from LEVs may cool the filament too fast, which might affect print quality. This research gap on positioning, distance, and capture velocity of LEV extends beyond FFF 3-D printers to all types of AM processes.

Ventilated enclosures that were retrofit to an FFF 3-D printer (Figure 5) had median efficacy of 97% and better controlled particle emissions compared with ventilated enclosures designed by the printer manufacturer (median efficacy of 52.6%). The precise reason(s) for the higher performance of retrofit ventilated enclosures was not clear from the literature. One possible explanation was that retrofit controls were likely implemented for the sole purpose of lowering emissions, whereas a manufacturer’s design might reflect a balance of multiple considerations (e.g., thermal stability of the build chamber atmosphere to produce a high-quality part, complexity of manufacturing a printer, and reduction of emissions). Isolation as an engineering control strategy generally displayed poor performance, but it was higher when designed by a manufacturer (median efficacy of 45%) compared with when it was retrofit (median efficacy of 33.4%) to an FFF 3-D printer. This observation was somewhat surprising given that earlier studies indicated that the efficacy of loose-fitting printer covers designed to maintain thermal stability of the build chamber atmosphere showed poor efficacy in controlling particle emissions (Azimi et al. 2016; Yi et al. 2016). The better performance of isolation controls designed by manufacturers might reflect the evolution in printer designs over time that now go beyond maintaining the build chamber temperature to containing contaminants; Runstrom Eden et al. (2022) and Viitanen et al. (2021) reported efficacies of modern printer enclosures exceeded 95%. The efficacy of ventilated enclosures, LEV, and isolation for particle emissions from FFF 3-D printers were similar or higher when assessed in test chamber settings compared with real-world settings (Figure 5). This finding suggested that test chambers were a reliable first step in the evaluation of engineering controls, but positive results in chamber studies need to

be verified by studies in real-world settings (the same verification should apply to all types of AM processes). Finally, it is worth noting that many ventilation control strategies included filtration media such as HEPA, poly-acrylonitrile nanofiber, electret/antibacterial, polyethylene, and nanomembrane filters to capture particles (Cao et al. 2019; Cao and Pui 2020; Dunn et al. 2020; Du Preez et al. 2018; Gu et al. 2019; HSE 2019; Katz et al. 2020; Kwon et al. 2017; Secondo et al. 2020; Stefaniak et al. 2019b; Viitanen et al. 2021); however, limited available data does not permit conclusion as to which type of filter provides the best capture performance for particles. The collection efficiency of a given type of filter depends on many factors, including the construction of the filter itself and characteristics of the particle such as size and electrostatic charge. Multiple published papers reported different capture efficiencies of filters for particles. Among these papers, only Kwon et al. (2017) systematically evaluated several types of filter media using the same experimental setup, but even then, collection efficiencies for particles ranged from 76.6% to 99.9%, which indicated that the characteristics of the particles and/or filter were important factors when designing controls.

Gases—When data from FFF 3-D and MJ printers were combined, the calculated median efficacy value for the engineering tier of the hierarchy of controls was 55.6%, but when data were parsed between printer types, the median efficacy value decreased to 23.9% for FFF 3-D printers and increased to 66.7% for MJ printers. Hence, the efficacy of engineering controls for gases emitted by FFF 3-D printers was poorer than initially concluded based upon combined data.

Within the engineering tier of the hierarchy, for FFF 3-D printers and MJ printers combined, the median efficacy of ventilation (LEV) to reduce gas-phase emissions was 69.4%. When data were parsed between printer types, the median efficacy decreased to 28.2% for FFF 3-D printers but remained similar at 71.4% for MJ printers. Hence, ventilation alone appears promising as an engineering control for gas-phase emissions from MJ printers, but more research is needed to improve the efficacy of this approach for FFF 3-D printers. Note that while ventilation alone had poor efficacy in controlling gas-phase emissions from FFF 3-D printers, similar to that for particles, isolation exhibited even less efficacy (median of 14.6%) compared with any type of ventilated control (LEV or ventilated enclosure). Several of the ventilation-based controls (LEV or ventilated enclosures) assessed in the literature for FFF 3-D printers also incorporated filter media into the design. Some examples of media were graphitic carbon nitride doped with metals (Wojtyła, Śpiewak, and Baran 2020), HEPA filters (Davis et al. 2019), and HEPA-HIMOP or HEPA-ACF combinations (Gu et al. 2019; Stefaniak et al. 2019b). One possible explanation for the relatively poor performance of ventilation-based controls to lower gas-phase emissions might be related to the findings of Gu et al. (2019) and Davis et al. (2019). Both research groups documented an increase in TVOC levels and levels of specific VOCs as well as the presence of new gas-phase emissions that were not present during printing without a filtered ventilation control in place. Davis et al. (2019) indicated that the source of these VOCs might have been the filter material itself. Gu et al. (2019) demonstrated that concentrations of VOCs decreased after the filter in the cover was conditioned and operated for a few days, which supported the premise that the HEPA filter contributed to gas-phase emissions. Future research on the

efficacy of filter-based controls for gas-phase emissions needs to consider the contribution of the media itself to contaminant levels. Available data were too sparse to permit conclusion as to whether any one type of filter provided the best capture performance for gases. There were no apparent data available to base guidance on the positioning, distance, and capture velocity of LEV relative to the printer (or extruder nozzle) for control of gas-phase emissions. Finally, data on the efficacy of engineering controls for gas-phase emissions were too sparse to permit comparison of results between test chamber and real-world settings; in the absence of more data, it seems prudent that promising results in test chambers need to be verified by studies in real-world settings.

Administrative controls

Administrative controls serve as changes in work practices. On their own, administrative controls may sometimes be difficult to implement and maintain, such that they are often used in conjunction with engineering controls and PPE to effectively control or eliminate a hazard. These controls are sometimes viewed as a short-term solution that is implemented while a hazard is removed or reduced using other control technologies. Findings from the investigations of administrative controls provided useful information that might easily be applied to the workplace, AM machine print parameters, and the AM machine setup.

Results of emissions monitoring in NF and FF locations for AM processes varied among three studies (Lewinski, Secondo, and Ferri 2019; Stefaniak et al. 2022; Zhou et al. 2015). Given the conflicting observations among these studies, when investigating NF and FF contaminant concentrations, factors such as the type of contaminant and the airflow patterns in the workplace area need to be taken into consideration using particle mapping and a CNC, visualizing airflow patterns using smoke tubes, or by other means. Both machine operators and bystanders need to be aware of potential for contaminant release in a space when undertaking specific tasks associated with an AM process and the printing step itself and that distance from an AM machine does not always confer a reduction in exposure.

Changes to print parameters might be an effective administrative control, which indicated that operating procedures, printer model, and feedstock material type need to be taken into consideration when conducting work (Cheng et al. 2018; Deng et al. 2016; Simon et al. 2018). AM operators are usually skilled engineers who also act as part designer and printer technician, and therefore with knowledge of the influence of certain print parameters on emissions, these individuals could proactively adjust print designs and printer settings to lower exposures. Furthermore, Simon et al. (2018) recommended that the extruder nozzle be properly cleaned after each run and that the filament needs to be retracted out of the extruder nozzle during the pre-heating step.

Both Wojnowski et al. (2020) and Khaki et al. (2021) concluded that the use of sensors might alert an AM machine operator of high emissions concentrations and the need to implement exposure mitigation steps. Another opportunity to incorporate sensors as administrative controls might be to monitor build quality during FFF 3-D printing. Minetola et al. (2022) applied an *in situ* monitoring system to detect possible print defects during the build cycle by comparing images of each build layer to the computer code for the print job. Although this monitoring system is intended to improve part quality, print

defects lead to a printer malfunction, which often results in higher particle emissions (Mendes et al. 2017; Stefaniak et al. 2019b; Yi et al. 2016), monitors could also serve as an administrative warning to not immediately approach a printer and thereby reduce exposures. Another example is the application of machine learning techniques to monitor 3-D printer performance to distinguish among various printing conditions (e.g., use of a clogged nozzle) to support quality assurance in AM (Westphal and Seitz 2021). In this study, investigators used an environmental monitoring sensor including air pressure, humidity, temperature, and VOCs during FFF 3-D printing. Air pressure was identified as the most influential environmental monitoring parameter and VOC levels were the least influential for input to the machine learning model (Westphal and Seitz 2021). Despite limited utility of VOC monitoring in this research as input to a machine learning model, if relationships between VOC levels and 3-D printer performance parameters (e.g., acoustic signals) can be identified, machine performance monitoring might be a useful administrative control.

Each AM process category is based upon a different principle of operation and therefore will have different process phases. Recognizing which controls are most relevant to a given AM process might assist in identifying and reducing occupational exposures beforehand (Bau et al. 2020; Dugheri et al. 2022; Han, Zhao, and Li 2021; Petretta et al. 2019). Some administrative controls might be viewed as short-term solutions (e.g., establishing zone control) but many might be effective in the long term if these are affordable and tailored to a specific AM process and workplace setup (e.g., adjusting print parameters to lower exposures and negate the need for zone control). When setting up administrative controls in a workplace, the following order of preference might be useful: area/setting (parameters) > filament (parameters) > machine (parameters) > workplace task specifics.

Personal protective equipment

Graff et al. (2017) found that the Sundström SR 500 as respiratory protective equipment was sufficient in removing particles when worn during PBF. However, their study only investigated respiratory protection against particles and not gases, nor were other forms of PPE evaluated such as protective clothing. Although Graff et al. (2017) was the only published paper identified by the literature search that evaluated respiratory protection from particles in an AM workplace, PPE has been extensively studied for gas- and particle-phase emissions from many other processes. Even though PPE occupies the lowest tier in our version of the hierarchy of controls, it might provide protection when coupled with existing facility-specific control measures that are tailored to the specific AM work environment. Therefore, there is still a need to establish the efficacy of the different types of PPE in reducing exposures to AM process emissions.

Summary

A search of the available literature identified 42 articles that met the inclusion criteria for this review. Data were available that quantified the efficacy of at least one control for all but the SL process category. More data were available on controls for particle emissions from AM processes compared with gas-phase emissions. The majority of available data on controls were for ME-type FFF 3-D printers, and to a lesser degree, MJ printers. In

the context of the hierarchy of controls, the paucity of available data precluded drawing firm conclusions on the efficacy of PtD, elimination, substitution, administrative, and PPE controls. Available data indicated that engineering controls for ME-type FFF 3-D printers that included LEV generally displayed higher efficacy in reducing particle and gas levels compared with isolation alone. Furthermore, efficacies of engineering controls for particle emissions from FFF 3-D printers appeared to be higher when evaluated in test chamber settings compared with real-world settings. As such, it seems prudent that positive results in test chambers need to be confirmed by studies in real-world settings. From this literature review, the following research gaps were identified:

- Data are needed on the efficacy of controls for emissions from all AM process categories, not just ME-type FFF 3-D printers and MJ printers.
- More data are needed to understand potential particle size-dependent effects on the efficacy of engineering controls.
- More data are needed to understand the efficacy of controls for gas-phase emissions, including control solutions that do not contribute to gaseous emissions as documented for some filter media.
- Future data collection for AM process emissions (particles and gases) should be conducted in a more standardized manner (type of instrument, metrics, etc.) to facilitate inter-comparison of results among studies.
- Existing studies on controls have focused exclusively on the inhalation exposure pathway, and there is currently no research on minimizing dermal exposures to resin and powder feedstocks.
- Within the context of our version of the hierarchy of controls:
  - Application of PtD concepts to AM processes is relatively nascent but shows promise for application of CFD modeling to the design of workplaces and opportunities exist to expand PtD to other areas such as feedstocks that control their own emissions.
  - More studies are needed to assess whether substitution of polymer feedstocks can provide opportunities to lower emissions compared with virgin polymers.
  - Improved understanding of engineering controls is needed, including which type of filter provides the best capture performance for aerosols and gases and the impact of positioning, distance, and capture velocity of LEV relative to a printer.
  - More studies are necessary to assess the efficacy of administrative controls, especially for task-based activities throughout AM processes.
  - PPE might be needed, but it is the least-preferred method. PPE should be used in combination with other control measures. However, more studies are needed to investigate the use of PPE in different AM

environments in terms of correct type of PPE selected, its correct use, maintenance/replacement, and storage.

Finally, it is important to note that for all control types, there is a need for regular maintenance and verification of their efficiency to ensure proper effectiveness.

Supplementary Material

Refer to Web version on PubMed Central for supplementary material.

Acknowledgments

The findings and conclusions in this report are those of the authors and do not necessarily represent the official position of the National Institute for Occupational Safety and Health, Centers for Disease Control and Prevention. Mention of any company or product does not constitute endorsement by the U.S. Government, National Institute for Occupational Safety and Health, or the Centers for Disease Control.

Funding

This work was supported by The South African Department of Science and Innovation through the Collaborative Programme in Additive Manufacturing. A.B.S was supported by NIOSH intramural research funds.

Data availability statement

All data is presented in Table 1 of this article.https//:doi.org/10.1080/10937404.2022.2092569

References

Aluri M, Monami B, Raj BS, and Mamilla RS. 2021. Review on particle emissions during fused deposition modeling of acrylonitrile butadiene styrene and polylactic acid polymers. Mater. Today Proc 44: 1375–83. doi: 10.1016/j.matpr.2020.11.521.

Azimi P, Zhao D, Pouzet C, Crain NE, and Stephens B. 2016. Emissions of ultrafine particles and volatile organic compounds from commercially available desktop three-dimensional printers with multiple filaments. Environ. Sci. Technol 50:1260–68. doi:10.1021/acs.est.5b04983. [PubMed: 26741485]

Azzougagh MN, Keller FX, Cabrol E, Cici M, and Pourchez J. 2021. Occupational exposure during metal additive manufacturing: A case study of laser powder bed fusion of aluminum alloy. J. Occup. Environ. Hyg 18:223–36. doi:10.1080/15459624.2021.1909055. [PubMed: 33989129]

Bau S, Rousset D, Payet R, and Keller FX. 2020. Characterizing particle emissions from a direct energy deposition additive manufacturing process and associated occupational exposure to airborne particles. J. Occup. Environ. Hyg 17:59–72. doi:10.1080/15459624.2019.1696969. [PubMed: 31829796]

Cao M, Gu F, Rao C, Fu J, and Zhao P. 2019. Improving the electrospinning process of fabricating nanofibrous membranes to filter PM2.5. Sci. Total Environ 666:1011–21. doi:10.1016/j.scitotenv.2019.02.207. [PubMed: 30970468]

Cao LNY, and Pui DYH. 2020. Real-time measurements of the particle geometric surface area by the weighted-sum method on a university campus. Aerosol Air Qual. Res 20:1569–81. doi:10.4209/aaqr.2019.12.0621.

Chan FL, House R, Kudla I, Lipszyc JC, Rajaram N, and Tarlo SM. 2018. Health survey of employees regularly using 3D printers. Occup. Med (Lond) 68:211–14. doi:10.1093/occmed/kqy042. [PubMed: 29538712]

Chan FL, Hon C-Y, Tarlo SM, Rajaram N, and House R. 2020. Emissions and health risks from the use of 3D printers in occupational settings. J. Toxicol. Environ. Health Part A . 83:279–87. doi:10.1080/15287394.2020.1751758.

Chang TY, Lee LJ, Wang JD, Shie RH, and Chan CC. 2004. Occupational risk assessment on allergic contact dermatitis in a resin model making process. J Occup Health 46:148–52. doi:10.1539/joh.46.148. [PubMed: 15090690]

Chen R, Yin H, Cole IS, Shen S, Zhou X, Wang Y, and Tang S. 2020. Exposure, assessment and health hazards of particulate matter in metal additive manufacturing: A review. Chemosphere 259:127452. doi:10.1080/15287394.2020.1751758. [PubMed: 32629313]

Cheng YL, Zhang LC, Chen F, and Tseng YH. 2018. Particle emissions of material-extrusion-type desktop 3D printing: The effects of infill. Int. J. Precis. Eng. Manuf. Green Technol 5:487–97. doi:10.1007/s40684-018-0052-3.

Creytens K, Gilissen L, Huygens S, and Goossens A. 2017. A new application for epoxy resins resulting in occupational allergic contact dermatitis: The three-dimensional printing industry. Contact. Derm 77:349–51. doi:10.1111/cod.12840.

Davis AY, Zhang Q, Wong JPS, Weber RJ, and Black MS. 2019. Characterization of volatile organic compound emissions from consumer level material extrusion 3D printers. Build. Environ 160:106209. doi:10.1016/j.buildenv.2019.106209.

De Almeida MMF, Henning HHW, Da Costa PF, Malda J, Le Gac S, Bray F, Van Duursen MBM, Brouwers JF, Van De Lest CHA, Bertijn I, et al. 2018. Potential health and environmental risks of three-dimensional engineered polymers. Environ. Sci. Technol. Lett 5:80–85. doi:10.1021/acs.estlett.7b00495. [PubMed: 29911125]

Deng Y, Cao SJ, Chen A, and Guo Y. 2016. The impact of manufacturing parameters on submicron particle emissions from a desktop 3D printer in the perspective of emission reduction. Build. Environ 104:311–19. doi:10.1016/j.buildenv.2016.05.021.

Ding S, and Ng BF. 2021. Particle emission levels in the user operating environment of powder, ink and filament-based 3D printers. Rapid Prototyping J. 27:1124–32. doi:10.1108/RPJ-02-2020-0039.

Du Preez S, Johnson A, LeBouf RF, Linde SJL, Stefaniak AB, and Du Plessis J. 2018. Exposures during industrial 3-D printing and post-processing tasks. Rapid Prototyping J. 24:865–71. doi:10.1108/RPJ-03-2017-0050.

Dugheri S, Cappelli G, Trevisani L, Kemble S, Paone F, Rigacci M, Bucaletti E, Squillaci S, Mucci N, and Arcangeli G. 2022. A qualitative and quantitative occupational exposure risk assessment to hazardous substances during powder-bed fusion processes in metal-additive manufacturing. AGRIS. 8:32. oai:mdpi.com: 1660-4601/19/9/4996.

Dunn KL, Hammond D, Menchaca K, Roth G, and Dunn KH. 2020. Reducing ultrafine particulate emission from multiple 3D printers in an office environment using a prototype engineering control. J. Nanopart. Res 22:112. doi:10.1007/s11051-020-04844-4.

Farcas MT, Stefaniak AB, Knepp AK, Bowers L, Mandler WK, Kashon M, Jackson SR, Stueckle TA, Sisler JD, Friend SA, et al. 2019. Acrylonitrile butadiene styrene (ABS) and polycarbonate (PC) filaments three-dimensional (3-D) printer emissions-induced cell toxicity. Toxicol. Lett 317:1–12. doi:10.1016/j.toxlet.2019.09.013. [PubMed: 31562913]

Farcas MT, McKinney W, Qi C, Mandler KW, Battelli L, Friend SA, Stefaniak AB, Jackson M, Orandle M, Winn A, et al. 2020. Pulmonary and systemic toxicity in rats following inhalation exposure of 3-D printer emissions from acrylonitrile butadiene styrene (ABS) filament. Inhal Toxicol 32:403–18. doi:10.1080/08958378.2020.1834034. [PubMed: 33076715]

Ford S 2014. Additive manufacturing technology: Potential implications for U.S. manufacturing competitiveness. J. Int. Commer. Econ. Policy 6:40–74.

Graff P, Stahlbom B, Nordenberg E, Graichen A, Johansson P, and Karlsson H. 2017. Evaluating measuring techniques for occupational exposure during additive manufacturing of metals: A pilot study. J. Ind. Ecol 21:S120–S129. doi:10.1111/jiec.12498.

Gu J, Wensing M, Uhde E, and Salthammer T. 2019. Characterization of particulate and gaseous pollutants emitted during operation of a desktop 3D printer. Environ. Int 123:476–85. doi:10.1016/j.envint.2018.12.014. [PubMed: 30622073]

Gumperlein I, Fischer E, Dietrich-Gumperlein G, Karrasch S, Nowak D, Jorres RA, and Schierl R. 2018. Acute health effects of desktop 3D printing (fused deposition modeling) using acrylonitrile butadiene styrene and polylactic acid materials: An experimental exposure study in human volunteers. Indoor Air 28:611–23. doi:10.1111/ina.12458. [PubMed: 29500848]

Han M, Zhao J, and Li L. 2021. Emissions of volatile organic compounds from 4D printing and associated control strategies towards workplace safety. Proceedings of ASME 2021: 16th International Manufacturing Science and Engineering Conference. doi: 10.1115/MSEC2021-63540.

Hayes AC, Osio-Norgaard J, Miller S, Whiting GL, and Vance ME. 2021. Air pollutant emissions from multi jet fusion, material-jetting, and digital light synthesis commercial 3D printers in a service bureau. Build. Environ 202:108008. doi: 10.1016/j.buildenv.2021.108008.

House R, Rajaram N, and Tarlo SM. 2017. Case report of asthma associated with 3D printing. Occup. Med (Lond) 67:652–54. doi:10.1093/occmed/kqx129. [PubMed: 29016991]

HSE. 2019. Measuring and controlling emissions from polymer filament desktop 3D printers. Buxton, UK: Health and Safety Executive.

ISO/ASTM. 2015. 52900: Additive manufacturing — General principles — Terminology. Geneva, Switzerland: ISO.

Jiang Q, Xu Y, Chen M, Meng Q, and Zhang C. 2021. Modification of the wood-plastic composite for enhancement of formaldehyde clearance and the 3D printing application. J. Appl. Polym. Sci 138:49683. doi:10.1002/app.49683.

Karayannis P, Petrakli F, Gkika A, and Koumoulos EP. 2019. 3D-printed lab-on-a-chip diagnostic systems-developing a safe-by-design manufacturing approach. Micromachines 10:825. doi:10.3390/mi10120825.

Katz EF, Goetz JD, Wang C, Hart JL, Terranova B, Taheri ML, Waring MS, and DeCarlo PF. 2020. Chemical and physical characterization of 3D printer aerosol emissions with and without a filter attachment. Environ. Sci. Technol 54:947–54. doi:10.1021/acs.est.9b04012. [PubMed: 31834782]

Khaki S, Duffy E, Smeaton AF, and Morrin A. 2021. Monitoring of particulate matter emissions from 3d printing activity in the home setting. Sensors 21:3247. doi:10.3390/s21093247. [PubMed: 34067219]

Kumar P, Robins A, Vardoulakis S, and Britter R. 2010. A review of the characteristics of nanoparticles in urban atmosphere and the prospects for developing regulatory controls. Atmos. Environ 44:5035–52. doi:10.1016/j.atmosenv.2010.08.016.

Kwon O, Yoon C, Ham S, Park J, Lee J, Yoo D, and Kim Y. 2017. Characterization and control of nanoparticle emission during 3D printing. Environ. Sci. Technol 51:10357–68. doi:10.1021/acs.est.7b01454. [PubMed: 28853289]

Leso V, Ercolano ML, Mazzotta I, Romano M, Cannavacciuolo F, and Iavicoli I. 2021. Three-dimensional (3D) printing: Implications for risk assessment and management in occupational settings. Ann. Work Exposures Health 65:617–34. doi:10.1093/annweh/wxaa146.

Lewinski NA, Secondo LE, and Ferri JK. 2019. On-site three-dimensional printer aerosol hazard assessment: Pilot study of a portable in vitro exposure cassette. Process Saf. Prog 38:e12030. doi:10.1002/prs.12030.

Lim JXY, and Pham QC. 2021. Automated post-processing of 3D-printed parts: Artificial powdering for deep classification and localisation. Virtual. Phys. Prototyp 16:333–46. doi:10.1080/17452759.2021.1927762.

López De Ipiña JM, Vaquero C, Egizabal A, Patelli A, and Moroni L. 2021. Safe-by-design strategies applied to scaffold hybrid manufacturing. Journal of Physics: Conference Series, Grenoble, France, 1953: 012009. doi: 10.1088/17426596/1953/1/012009.

MacCuspie RI, Hill WC, Hall DR, Korchevskiy A, Strode CD, Kennedy AJ, Ballentine ML, Rycroft T, and Hull MS. 2021. Prevention through design: Insights from computational fluid dynamics modeling to predict exposure to ultrafine particles from 3D printing. J. Toxicol. Environ. Health Part A 84:458–74. doi:10.1080/15287394.2021.1886210.

Macdonald NP, Zhu F, Hall CJ, Reboud J, Crosier PS, Patton EE, Wlodkowic D, and Cooper JM. 2016. Assessment of biocompatibility of 3D printed photopolymers using zebrafish embryo toxicity assays. Lab. Chip 16:291–97. doi:10.1039/c5lc01374g. [PubMed: 26646354]

Mendes L, Kangas A, Kukko K, Mølgaard B, Säämänen A, Kanerva T, Flores Ituarte I, Huhtiniemi M, Stockmann-Juvala H, Partanen J, et al. 2017. Characterization of emissions from a desktop 3D printer. J. Ind. Ecol, 21(Suppl1):S94–S106. doi:10.1111/jiec.12569.

Minetola P, Khandpur MS, Iuliano L, Calignano F, Galati M, and Fontana L. 2022. In-situ monitoring for open low-cost 3D printing. In Lecture notes in mechanical engineering, ed. Argawal RK, 49–56. Singapore: Springer Nature Singapore Pte Ltd. doi:10.1007/978-981-16-3934-0_7.

Mylläri V, Hartikainen S, Poliakova V, Anderson R, Jönkkäri I, Pasanen P, Andersson M, and Vuorinen J. 2016. Detergent impurity effect on recycled HDPE: Properties after repetitive processing. J. Appl. Polym. Sci 133:43766–43766. doi:10.1022/app.43766.

NIOSH. Hierarchy of Controls 2015 [cited September 22, 2021. Available from https://www.cdc.gov/niosh/topics/hierarchy/default.html.

Oberbek P, Kozikowski P, Czarnecka K, Sobiech P, Jakubiak S, and Jankowski T. 2019. Inhalation exposure to various nanoparticles in work environment—contextual information and results of measurements. J. Nanopart. Res 21:222. doi:10.1007/s11051-019-4651-x.

Oddone E, Pernetti R, Fiorentino ML, Grignani E, Tamborini D, Alaimo G, Auricchio F, Previtali B, and Imbriani M. 2021. Particle measurements of metal additive manufacturing to assess working occupational exposures: A comparative analysis of selective laser melting, laser metal deposition and hybrid laser metal deposition. Ind. Health. Advpub doi:10.2486/indhealth.2021-0114.

Oskui SM, Diamante G, Liao C, Shi W, Gan J, Schlenk D, and Grover WH. 2016. Assessing and reducing the toxicity of 3D-printed parts. Environ. Sci. Technol. Lett 3:1–6. doi:10.1021/acs.estlett.5b00249.

Petretta M, Desando G, Grigolo B, and Roseti L. 2019. 3D printing of musculoskeletal tissues: Impact on safety and health at work. J. Toxicol. Environ. Health Part A 82:891–912. doi:10.1080/15287394.2019.1663458.

Popov VK, Evseev AV, Ivanov AL, Roginski VV, Volozhin AI, and Howdle SM. 2004. Laser stereolithography and supercritical fluid processing for custom-designed implant fabrication. J Mater Sci Mater Med 15:123–28. doi:10.1023/B:JMSM.0000011812.08185.2a. [PubMed: 15330045]

Potter PM, Al-Abed SR, Lay D, and Lomnicki SM. 2019. VOC emissions and formation mechanisms from carbon nanotube composites during 3Dprinting. Environ. Sci. Technol 53:4364–70. doi:10.1021/acs.est.9b00765. [PubMed: 30875473]

Runstrom Eden G, Tinnerberg H, Rosell L, Moller R, Almstrand AC, and Bredberg A. 2022. Exploring methods for surveillance of occupational exposure from additive manufacturing in four different industrial facilities. Ann. Work Exposures Health 66:163–77. doi:10.1093/annweh/wxab070.

Secondo LE, Adawi HI, Cuddehe J, Hopson K, Schumacher A, Mendoza L, Cartin C, and Lewinski NA. 2020. Comparative analysis of ventilation efficiency on ultrafine particle removal in university makerspaces. Atmos. Environ 224:117321. doi:10.1016/j.atmosenv.2020.117321.

Simon TR, Lee WJ, Spurgeon BE, Boor BE, and Zhao F. 2018. An experimental study on the energy consumption and emission profile of fused deposition modeling process. Procedia Manuf. 26:920–28. doi:10.1016/j.promfg.2018.07.119.

Singh AV, Maharjan RS, Jungnickel H, Romanowski H, Hachenberger YU, Reichardt P, Bierkandt F, Siewert K, Gadicherla A, Laux P, et al. 2021. Evaluating particle emissions and toxicity of 3D pen printed filaments with metal nanoparticles as additives: *In vitro* and *in silico* discriminant function analysis. ACS Sustain. Chem. Eng 9:11724–37. doi:10.1021/acssuschemeng.1c02589.

Stefaniak AB, LeBouf RF, Duling MG, Yi J, Abukabda AB, McBride CR, and Nurkiewicz TR. 2017a. Inhalation exposure to three-dimensional printer emissions stimulates acute hypertension and microvascular dysfunction. Toxicol. Appl. Pharmacol 335:1–5. doi:10.1016/j.taap.2017.09.016. [PubMed: 28942003]

Stefaniak AB, LeBouf RF, Yi J, Ham JE, Nurkewicz TR, Schwegler-Berry DE, Chen BT, Wells JR, Duling MG, Lawrence RB, et al. 2017b. Characterization of chemical contaminants generated by a desktop fused deposition modeling 3-dimensional printer. J. Occup. Environ. Hyg 14:540–50. doi:10.1080/15459624.2017.1302589. [PubMed: 28440728]

Stefaniak AB, Johnson AR, du Preez S, Hammond DR, Wells JR, Ham JE, LeBouf RF, Martin SB Jr., Duling MG, Bowers LN, et al. 2019a. Insights into emissions and exposures from use

of industrial-scale additive manufacturing machines. Saf Health Work 10:229–36. doi:10.1016/j.shaw.2018.10.003. [PubMed: 31297287]

Stefaniak AB, Johnson AR, du Preez S, Hammond DR, Wells JR, Ham JE, LeBouf RF, Menchaca KW, Martin MGDSB Jr, Bowers LN, et al. 2019b. Evaluation of emissions and exposures at workplaces using desktop 3-dimensional printers. J. Chem. Health Saf 26:19–30. doi:10.1016/j.jchas.2018.11.001. [PubMed: 31798757]

Stefaniak AB, Du Preez S, and Du Plessis JL. 2021a. Additive manufacturing for occupational hygiene: A comprehensive review of processes, emissions, and exposures. J. Toxicol. Environ. Health B 24:173–222. doi:10.1080/10937404.2021.1936319.

Stefaniak AB, Bowers LN, Cottrell G, Erdem E, Knepp AK, Martin SB Jr., Pretty J, Duling MG, Arnold ED, Wilson Z, et al. 2021b. Use of 3-dimensional printers in educational settings: The need for awareness of the effects of printer temperature and filament type on contaminant releases. ACS Chem. Health Saf 28:444–56. doi:10.1021/acs.chas.1c00041.

Stefaniak AB, Bowers L, Martin SB, Hammond JD, Ham JE, Wells JR, Fortner AR, Knepp AK, du Preez S, Pretty J, et al. 2021c. Large format additive manufacturing and machining using High melt temperature polymers. Part I: Real-time particulate and gas-phase eissions. ACS Chem. Health Saf 28:190–200. doi:10.1021/acs.chas.0c00128.

Stefaniak AB, Bowers LN, Cottrell G, Erdem E, Knepp AK, Martin SB Jr., Pretty J, Duling MG, Arnold ED, Wilson Z, et al. 2022. Towards sustainable additive manufacturing: The need for awareness of particle and vapor releases during polymer recycling, making filament, and fused filament fabrication 3-D printing. Resour. Conserv. Recycl 176:105911. doi:10.1016/j.resconrec.2021.105911.

Stephens B, Azimi P, El Orch Z, and Ramos T. 2013. Ultrafine particle emissions from desktop 3D printers. Atmos. Environ 79:334–39. doi:10.1016/j.atmosenv.2013.06.050.

Väisänen AJK, Alonen L, Ylönen S, Lyijynen I, and Hyttinen M. 2021. The impact of thermal reprocessing of 3D printable polymers on their mechanical performance and airborne pollutant profiles. J. Polym. Res 28:436. doi:10.1007/s10965-021-02723-7.

Väisänen A, Alonen L, Ylönen S, and Hyttinen M. 2022. Organic compound and particle emissions of additive manufacturing with photopolymer resins and chemical outgassing of manufactured resin products. J. Toxicol. Environ. Health Part A 85:198–216. doi:10.1080/15287394.2021.1998814.

Vallabani NVS, Alijagic A, Persson A, Odnevall I, Sarndahl E, and Karlsson HL. 2022. Toxicity evaluation of particles formed during 3D-printing: Cytotoxic, genotoxic, and inflammatory response in lung and macrophage models. Toxicology 467:153100. doi:10.1016/j.tox.2022.153100. [PubMed: 35032623]

Viitanen AK, Uuksulainen S, Koivisto AJ, Hämeri K, and Kauppinen T. 2017. Workplace measurements of ultrafine particles - A literature review. Ann. Work Exposures Health 61:749–58. doi:10.1093/annweh/wxx049.

Viitanen AK, Kallonen K, Kukko K, Kanerva T, Saukko E, Hussein T, Hämeri K, and Säämänen A. 2021. Technical control of nanoparticle emissions from desktop 3D printing. Indoor Air 31:1061–71. doi:10.1111/ina.12791. [PubMed: 33647162]

Westphal E, and Seitz H. 2021. A machine learning method for defect detection and visualization in selective laser sintering based on convolutional neural networks. Addit. Manuf 41:101965. doi:10.1016/j.addma.2021.102535.

Wilkins DF, Traum MJ, and Wilkins-Earley JG. 2020. Teaching space-borne recycling to middle school students via 3d printing – Managing classroom air quality. AIAA Scitech 1:1–14. doi:10.2514/6.2020-0330.

Wojnowski W, Kalinowska K, Gębicki J, and Zabiegała B. 2020. Monitoring the BTEX volatiles during 3D printing with acrylonitrile butadiene styrene (ABS) using electronic nose and proton transfer reaction mass spectrometry. Sensors (Basel) 20:5531. doi:10.3390/s20195531.

Wojtyła S, Śpiewak K, and Baran T. 2020. Synthesis, characterization and activity of doped graphitic carbon nitride materials towards photocatalytic oxidation of volatile organic pollutants emitted from 3D printer. J. Photochem. Photobiol. A Chem 391:112355. doi:10.1016/j.jphotochem.2020.112355.

Yang Y, and Li L. 2018. Total volatile organic compound emission evaluation and control for stereolithography additive manufacturing process. J. Clean. Prod 170:1268–78. doi:10.1016/j.jclepro.2017.09.193.

Yi J, LeBouf RF, Duling MG, Nurkiewicz TR, Chen BT, Schwegler-Berry D, Virji MA, and Stefaniak AB. 2016. Emission of particulate matter from a desktop three-dimensional (3-D) printer. J. Toxicol. Environ. Health Part A . 79:453–65. doi:10.1080/15287394.2016.1166467.

Zhang Y, Jarosinski W, Jung Y-G, and Zhang J. 2018. Additive manufacturing processes and equipment. In Additive manufacturing, ed. Zhang J, and Jung Y-G, 39–51. Oxford: Butterworth-Heinemann.

Zhang Q, Pardo M, Rudich Y, Kaplan-Ashiri I, Wong JPS, Davis AY, Black MS, and Weber RJ. 2019. Chemical composition and toxicity of particles emitted from a consumer-level 3D printer using various materials. Environ. Sci. Technol 53:12054–61. doi:10.1021/acs.est.9b04168. [PubMed: 31513393]

Zhou Y, Kong X, Chen A, and Cao S. 2015. Investigation of ultrafine particle emissions of desktop 3D printers in the clean room. Procedia Eng. 121:506–12. doi:10.1016/j.proeng.2015.08.1099.

Zontek TL, Ogle BR, Jankovic JT, and Hollenbeck SM. 2017. An exposure assessment of desktop 3D printing. J. Chem. Health Saf 24:15–25. doi:10.1016/j.jchas.2016.05.008.

Zontek TL, Scotto N, and Hollenbeck S. 2021. Controls for university fabrication laboratories - Best practices for health and safety. J. Chem. Health Saf 28:119–28. doi:10.1021/acs.chas.0c00093.

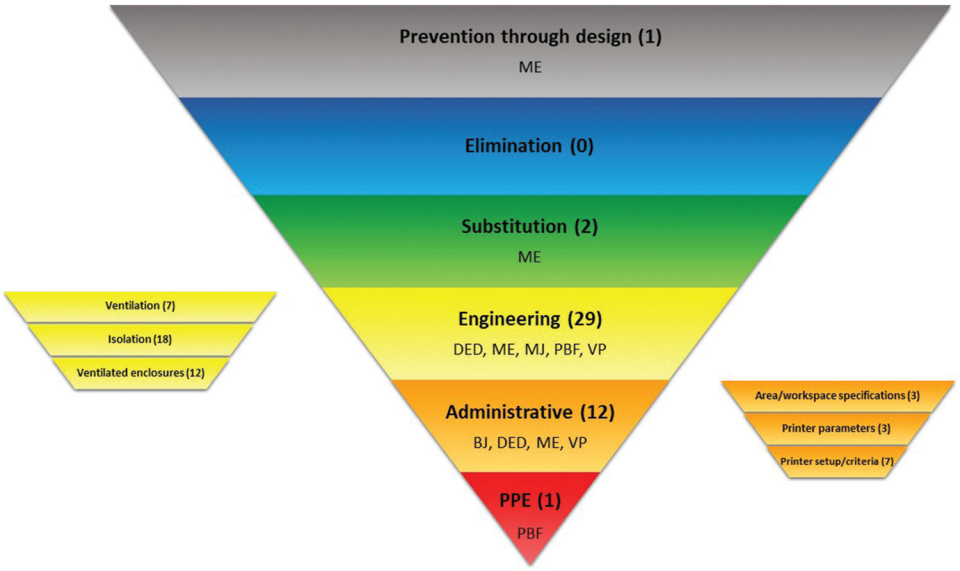

Figure 1.

Tested controls organized according to our version of the hierarchy of controls and additive manufacturing (AM) process category. The number of published articles for each tier is indicated in parentheses. Sub-classification of the engineering and administrative control tiers is also indicated. Note that the total number of articles given in Figure 1 (45) was greater than the total number of citations that met the inclusion criteria of this review (42) because some citations included results for more than one control type. ME = material extrusion, DED = directed energy deposition, MJ = material jetting, PBF = powder bed fusion, VP = vat photopolymerization, and BJ = binder jetting.

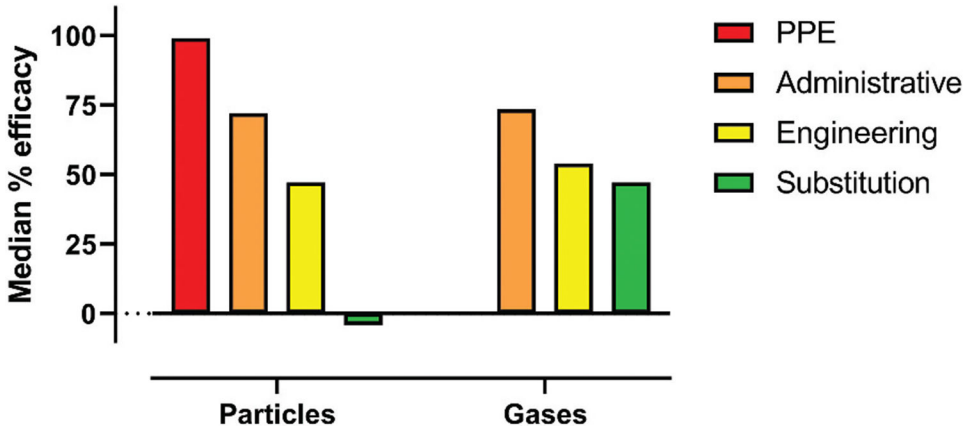

Figure 2.

Median % efficacies of controls for particle (n = 148 values) and gas emissions (n = 68 values) for all AM process categories by hierarchy tier.

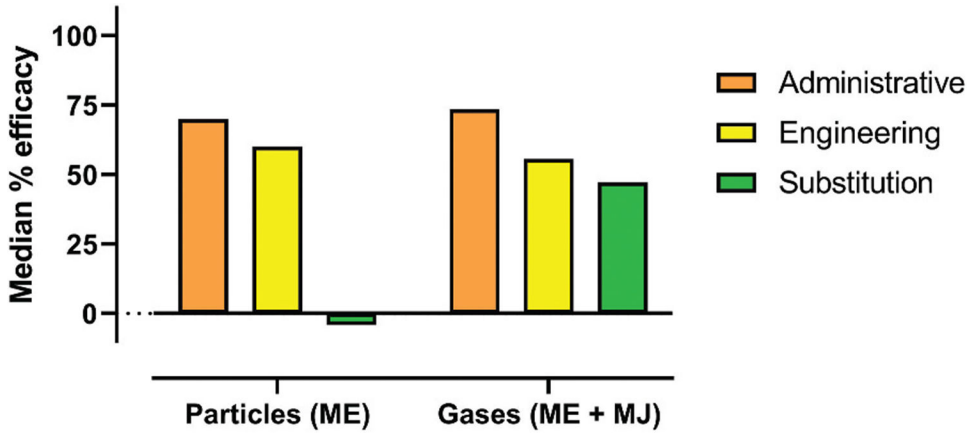

Figure 3.

Median % efficacies of controls for particle number-based data only (n = 94 values) and gas emissions (n = 58 values) for select AM processes by hierarchy tier. ME = FFF 3-D printers, MJ = material jetting.

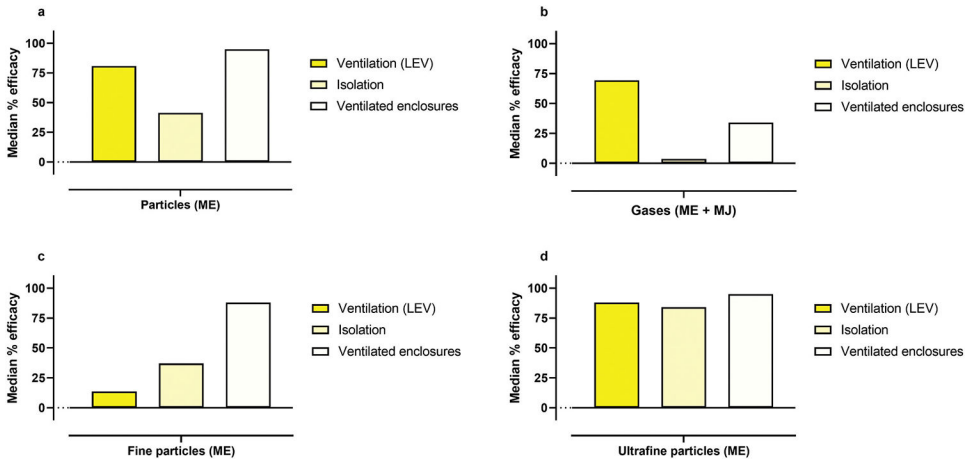

Figure 4.

Median % efficacies of controls for particle and gas emissions for select AM processes by type of engineering control: (a) medians for particles calculated from number-based data only (n = 65 values), (b) medians for gases calculated from all sample data (n = 51), (c) medians for particles calculated for fine size fraction only (n = 38 values), and (d) medians for particles calculated for ultrafine size fraction only (n = 24 values). ME = material extrusion (FFF 3-D printers only), MJ = material jetting.

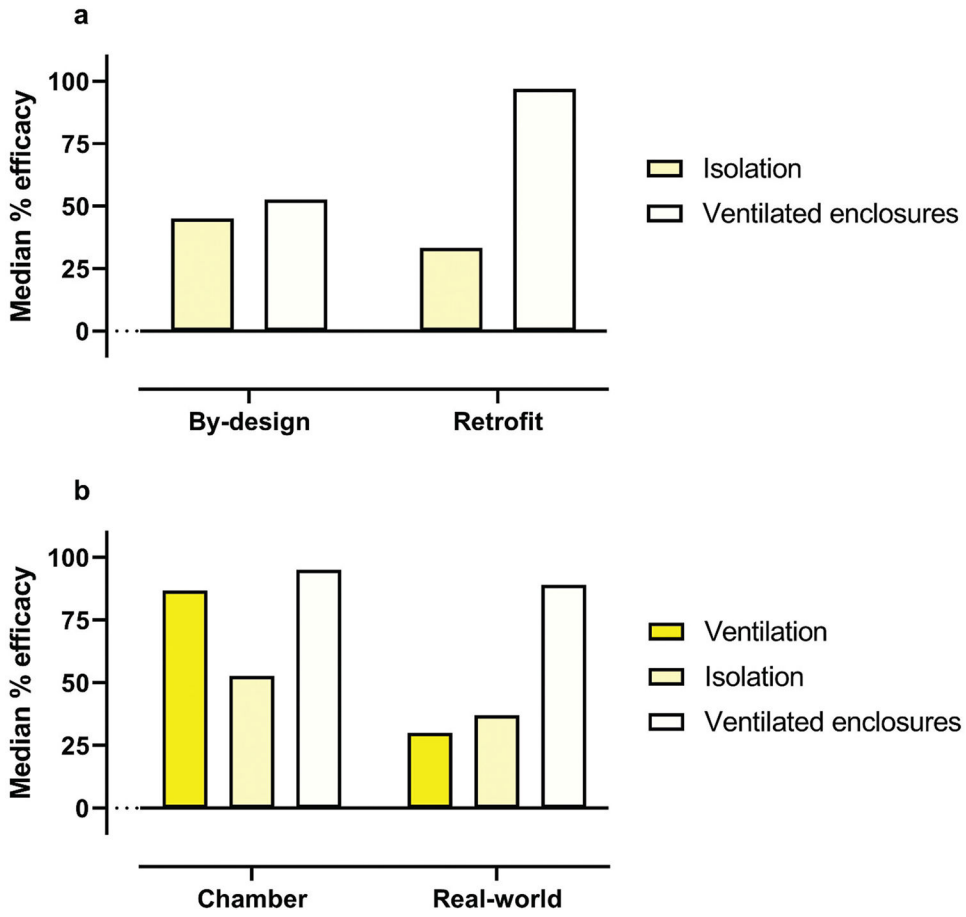

Figure 5.

Median % efficacies of engineering controls for particle number-based data only (n = 65 values) from material extrusion-type FFF 3-D printers by: (a) implemented by-design or retrofit, and (b) studied in a test chamber or real-world setting.

Table 1.

Efficacy of control technologies for additive manufacturing processes organized by hierarchy category (efficacy values in *italic* font were calculated by authors of this review from data given in the cited paper. Values in plain font were as given in the cited paper).

Citation	Process[a]	Setting	Details[b]	Control[c]	Metric[d]	Efficacy (%)[e]
Prevention-through-design						
MacCuspie et al. (2021)	ME (FFF)	Test chamber/Clean room	• TAZ 6 (Lulzbot) • Open frame • ABS filament	• CFD modeling for proactive design of workspaces	SMPS (#)[10–420 nm] OPS (#)[0.3–25 μm] Cyclone (m)[D_{50} = 4 μm]	Validated CFD model
Elimination						
n/a	n/a	n/a	• n/a	• n/a	n/a	n/a
Substitution						
Stefaniak et al. (2021b)	ME (FFF)	Teaching lab room	• Unspecified model/manufacturer • Open frame • PLA filaments	• Substitution of virgin PLA with recycled PLA filament (green) – “hot” printing	FMPS (#)[5.6–560 nm] CNC (#) [20–1000 nm] PID (TVOC)	*−89.2* *8.6* *40.8*
	ME (FFF)	Teaching lab room	• Unspecified model/manufacturer • Open frame • PLA filaments	• Substitution of virgin PLA with recycled PLA filament (gray) – “hot” printing	FMPS (#)[5.6–560 nm]CN C (#)[20–1000 nm] PID (TVOC)	*−39.3* *−110.5* *24.6*
	ME (FFF)	Teaching lab room	• Unspecified model/manufacturer • Open frame • ABS filaments	• Substitution of virgin ABS with recycled ABS filament – “normal” printing	FMPS (#)[5.6–560 nm] CNC (#) [20–1000 nm] PID (TVOC)	*15.9* *−186.0* *55.5*
	ME (FFF)	Teaching lab room	• Unspecified model/manufacturer • Open frame • ABS filaments	• Substitution of virgin ABS with recycled ABS filament – “hot” printing	FMPS (#)[5.6–560 nm] CNC (#) [20–1000 nm] PID (TVOC)	*56.7* *77.7* *53.5*
Väisänen et al. (2021)	ME (FFF)	Lab room	• Zmorph 2.0 SX (Zmorph S.A.) • Fully enclosed	• Substitution of virgin PLA with recycled PLA filament	CNC (#) [20–1000 nm] Baseline	 *15.7*

Citation	Process[a]	Setting	Details[b]	Control[c]	Metric[d]	Efficacy (%)[e]
			• PLA filaments		TC 1	*1.2*
					TC 2	*26.3*
					TC 3	*45.0*
					TC 4	*−9.5*
					TC 5	*25.0*
	ME (FFF)	Lab room	• ZMorph 2.0 SX (ZMorph S.A.) • Fully enclosed • PP filaments	• Substitution of virgin PP with recycled PP filament	CNC (#) [20–1000 nm]	
					Baseline	*−129.3*
					TC 1	*−264.4*
					TC 2	*−497.9*
					TC 3	*−775.3*
Engineering						
Oddone et al. (2021)	DED	Workplace	• Six-axis robotic arm (unspecified model/ manufacturer) • Freely moving • Stainless steel 316 and Inconel 718 powders	• Ventilated enclosure (retrofit) – full enclosure w/LEV	Inhalable (m):[D_{50} = 100 μm]	
					Chromium	*28.6*
					Cobalt	*70.8*
					Nickel	*34.0*
					Iron	*16.7*
Runstrom Eden et al. (2022)	ME (FFF)	Workplace	• Three printers (n = 2 Ultimaker 3; n = 1 Ultimaker 5) enclosed with hoods (unspecified material) • Ultimaker 3 • Side walls but no top or front • TPU, tough PLA, PET-CF, PC, ABS filaments • Ultimaker 5 • Side walls and split front doors but no top • TPU, tough PLA, PET-CF, PC, ABS filaments	• Isolation (retrofit) – full enclosure	CNC (#) [20–1000 nm]	*98* [≠,∩,B]
Väisänen et al. (2022)	MJ	Lab room	• Model J735 (Stratasys) • Fully enclosed with hinged cover	• Ventilation (by design) – built-in LEV (7 ACH)	CNC (#) [7–3000 nm]	*62.1*
					TD tube (m): Isob. acrylate	*98.1*

Citation	Process[a]	Setting	Details[b]	Control[c]	Metric[d]	Efficacy (%)[e]
			• VeroCyan-V, VeroMagenta-V, VeroYellow-V, VeroPureWhite, and VeroClear ink-like resins		IPA	*95.7*
					Σ(VOCs)	*97.6*
					DNPH (m): Acetald.	*57.1*
					Acetone	*36.4*
					Benzald.	*37.5*
					2-Butanone	*75.0*
					Butyrald.	*50.0*
					Formald.	*40.0*
					Hexald.	*42.9*
					Propionald.	*66.7*
					Σ(Carbonyls)	*44.2*
	MJ	Lab room	• Model J735 (Stratasys) • Fully enclosed with hinged cover • VeroBlack Plus resin	• Ventilation (by design) – built-in LEV (7 ACH)	CNC (#) [7–3000 nm]	*68.6*
					TD tube (m):Isob. acrylate	*98.9*
					Prop. glycol	*96.7*
					Σ(VOCs)	*96.8*
					DNPH (m): Acetald.	*71.4*
					Acetone	*75.0*
					Butyrald.	*57.1*
					Formald.	*35.3*
					Hexald.	*55.6*
					Propionald.	*75.0*
					Σ(Carbonyls)	*57.9*
Azzougagh et al. (2021)	PBF (SFM)	Workplace	• ProX200 (3D Systems) • Sealed machine doors • Aluminum alloy powder	• Isolation (by design) – fully enclosed machine	CNC (#)[10–1000 nm]	*90.0*
Han, Zhao, and Li (2021)	VP (SLA)	Lab room	• Moai 130 (Peopoly) • Fully enclosed (non-airtight)	• Isolation (retrofit) – activated carbon absorbent bed placed inside enclosure	PID (TVOC)	58.9

Citation	Process[a]	Setting	Details[b]	Control[c]	Metric[d]	Efficacy (%)[e]
			• Methacrylate-based resin			
López De Ipiña et al. (2021)	ME (FFF)	Lab room	• FAST prototype printer/plasma jetting machine • Machine (open frame) enclosed in PMMA box (air-airtightness not specified) • PEOT/PBT polymer • PEOT/PBT w/rGO • PEOT/PBT w/HA	• Isolation (retrofit) – full enclosure[!!]	CNC (#)[10–1000 nm]	*13.2 to 32.5* *−11.3 to 34.5* *34.2 to 48.2*
	ME (FFF)	Lab room	• FAST prototype printer/plasma jetting machine • Machine (open frame) enclosed in PMMA box (air-airtightness not specified) • PEOT/PBT • PEOT/PBT w/rGO • PEOT/PBT w/HA	• Isolation (retrofit) – full enclosure[!!]	OPS (#)[0.3–10 μm]	*7.1 to 64.7* *60.0 to 82.1* *−18.4 to 20.0*
	ME (FFF) – plasma jetting post-printing task	Lab room	• FAST prototype printer/plasma jetting machine • Machine (open frame) enclosed in PMMA box (air-airtightness not specified) • PEOT/PBT • PEOT/PBT w/rGO • PEOT/PBT w/HA	• Ventilated enclosure (retrofit) – full enclosure w/LEV	CNC (#)[10–1000 nm]	*98.2 to 98.6* *97.8 to 98.6* *97.1 to 98.6*
	ME (FFF) – plasma jetting post-printing task	Lab room	• FAST prototype printer/plasma jetting machine • Machine (open frame) enclosed in PMMA box (air-airtightness not specified) • PEOT/PBT • PEOT/PBT w/rGO • PEOT/PBT w/HA	• Ventilated enclosure (retrofit) – full enclosure w/LEV	OPS (#)[0.3–10 μm]	*71.4 to 84.9* *91.9 to 95.7* *53.5 to 63.0*

Citation	Process[a]	Setting	Details[b]	Control[c]	Metric[d]	Efficacy (%)[e]
Stefaniak et al. (2021c)	ME (LFAM)	Workplace	• Models 603 and 606 (Cincinnati Inc.) • Machines (side walls but open tops) enclosed using custom-built canopies • ABS, PC, Ultem®, PPS, PSU pellets	• Isolation (retrofit) – full enclosure	CNC (#) [20–1000 nm] PID (TVOC)	*−313.6 to 77.8* *−925.0 to 58.8*
Viitanen et al. (2021)	ME (FFF)	Office	• Model 3 Education Edition (miniFactory) • Back wall but no side walls or top • ABS filament	• Ventilation (retrofit) – LEV canopy hood w/ HEPA filter positioned over printer nozzle	SMPS (#)[2–64 nm] DC (sa)[10–1000 nm]	30 49
	ME (FFF)	Office	• Model 3 Education Edition (miniFactory) • Printer (back wall but no side walls or top) enclosed in plastic (unspecified type) box with non-airtight door • ABS filament	• Isolation (retrofit) – full enclosure	SMPS (#)[2–64 nm] DC (sa)[10–1000 nm]	97 89
	ME (FFF)	Office	• Model 3 Education Edition (miniFactory) • Printer (back wall but no side walls or top) enclosed in plastic (unspecified type) box with non-airtight door • ABS filament	• Ventilated enclosure (retrofit) – full enclosure w/LEV	SMPS (#)[2–64 nm] DC (sa)[10–1000 nm]	99 96
Zontek, Scotto, and Hollenbeck (2021)	ME (FFF)	Fab Lab room	• Unspecified model/manufacturer (n = 8) • Open front • PLA filament	• Ventilation (retrofit) – LEV ducts positioned near printers	CNC (#)[10–1000 nm] OPS (m)[0.3–10 μm]	*13.6*[B] *42.3*[B]
Cao and Pui (2020)	ME (FDM™)	University room	• Dimension 1200es (Stratasys) • Sealed machine doors • ABS filament	• Ventilated enclosure (by design) – fully enclosed machine w/recirculating HEPA filter	SMPS (sa) [−]*SMPS (m) [−]*	*99*≠[B] *99.9*≠[B]
Dunn et al. (2020)	ME (FFF)	Office	• Replicator+ (MakerBot) • Side walls but no top • Tough PLA filament	• Ventilation (retrofit) – LEV nozzle hood w/ HEPA filter (1 printer)	SMPS (#)[10–420 nm]	98.0[B]
Katz et al. (2020)	ME (FFF)	Office	• H-800 (Afinia) • Hinged cover (non-airtight)	• Ventilated enclosure (by design) – fully enclosed	SMPS (#)[15–685 nm] m-AMS (m)[30–1000 nm]	*94.7* *91.1*

Citation	Process[a]	Setting	Details[b]	Control[c]	Metric[d]	Efficacy (%)[e]
			• ABS filament	machine w/recirculating HEPA filter		
Secondo et al. (2020)	ME (FFF)	Library MakerSpace	• Replicator 5th Gen. (MakerBot) • Side walls but no top • PLA filament	• Ventilation – GEV (3.1 ACH)	SMPS (#)[10–420 nm]/OPS (#) [0.3–10 μm]	−1.1 *[B]*
	ME (FFF)	Library MakerSpace	• Ultimaker 2 (Ultimaker) • Side walls but no top or front • PLA filament	• Ventilation – GEV (3.1 ACH)	SMPS (#)[10–420 nm]/OPS (#) [0.3–10 μm]	−627.9 *[B]*
	ME (FFF)	Library MakerSpace	• TAZ 5 (Lulzbot) • Open frame • PLA filament	• Ventilation – GEV (3.1 ACH)	SMPS (#)[10–420 nm]/OPS (#) [0.3–10 μm]	59.1 *[B]*
	ME (FFF)	Library MakerSpace	• TAZ 5 (Lulzbot) • Open frame • ABS filament	• Ventilation – GEV (3.1 ACH)	SMPS (#)[10–420 nm]/OPS (#) [0.3–10 μm]	−5.4 *[B]*
	ME (FFF)	Library MakerSpace	• TAZ 5 (Lulzbot) • Open frame • HIPS filament	• Ventilation – GEV (3.1 ACH)	SMPS (#)[10–420 nm]/OPS (#) [0.3–10 μm]	−31.6 *[B]*
	ME (FFF)	Library MakerSpace	• Replicator 5th Gen., Ultimaker 2, TAZ5 (Lulzbot) and laser cutter (w/fume extractor) operating simultaneously • PLA filaments	• Ventilation – GEV (3.1 ACH)	SMPS (#)[10–420 nm]/OPS (#) [0.3–10 μm]	−326.0 *[B]*
	ME (FFF)	Lab MakerSpace room	• 29 printers (n = 26 Replicator 5th Gen.; n = 1 Replicator+; n = 2 Ultimaker 3 Extended) enclosed in cabinets with non-airtight doors • Replicator 5th Gen. (MakerBot) • Side walls but no top • PLA filament • Replicator+ (MakerBot)	• Isolation (retrofit) – full enclosure using cabinets	SMPS (#)[10–420 nm]/OPS (#) [0.3–10 μm]	−9.8 to −70.1 *[B]*

Citation	Process[a]	Setting	Details[b]	Control[c]	Metric[d]	Efficacy (%)[e]
			• Side walls but no top • PLA filament • Ultimaker 3 Extended (Ultimaker) • Side walls but no top or front • PLA filament			
	ME (FFF)	Lab MakerSpace room	• 29 printers (n = 26 Replicator 5th Gen.; n = 1 Replicator+; n = 2 Ultimaker 3 Extended) enclosed in cabinets with non-airtight doors • Replicator 5th Gen. (MakerBot) • Side walls but no top • PLA filament • Replicator+ (MakerBot) • Side walls but no top • PLA filament • Ultimaker 3 Extended (Ultimaker) • Side walls but no top or front • PLA filament	• Ventilation – GEV (8.7 ACH) – cabinet enclosure doors open	SMPS (#)[10–420 nm]/OPS (#) [0.3–10 μm]	−64.9[B]
	ME (FFF)	CenterMakerSpace	• Replicator 5th Gen. (MakerBot) • Side walls but no top • PLA filament	• Ventilation – GEV (0.2 ACH)	SMPS (#)[10–420 nm]/OPS (#) [0.3–10 μm]	−1378.2[B]
	ME (FFF)	CenterMakerSpace	• UpBox+ (Beijing Tiertime) • Side walls and non-airtight cover • ABS filament	• Ventilation – GEV (0.2 ACH)	SMPS (#)[10–420 nm]/OPS (#) [0.3–10 μm]	−411.0[B]
	ME (FFF)	CenterMakerSpace	• Replicator 5th Gen. (n = 3) with PEA filament and UpBox+ (n = 1) with ABS filament operating simultaneously	• Ventilation – GEV (0.2 ACH)	SMPS (#)[10–420 nm]/OPS (#) [0.3–10 μm]	−4826.1[B]
	ME (FFF)	CenterMakerSpace	• Replicator 5th Gen. (n = 3) with PLA filament and UpBox+ (n = 1) with ABS filament operating simultaneously	• Ventilation (retrofit) – portable HEPA-ACF	SMPS (#)[10–420 nm]/OPS (#) [0.3–10 μm]	−1752.5[B]

Citation	Process[a]	Setting	Details[b]	Control[c]	Metric[d]	Efficacy (%)[e]
				positioned at printer exhaust		
Wilkins, Traum, and Wilkins-Earley (2020)	ME (FFF)	Classroom	• i3 MK3S (Prusa Research) • Printer (open frame) enclosed in PMMA box with doors (non-airtight) • ABS filament • PLA filament • PETG filament	• Isolation (retrofit) – full enclosure	OPS [PM_{10}] (m) [0.3–10 μm]	*24.3–77.1* *−53.4*
	ME (FFF)	Classroom	• i3 MK3S (Prusa Research) • Printer (open frame) enclosed in PMMA box with doors (non-airtight) • ABS filament • PLA filament • PETG filament	• Isolation (retrofit) – full enclosure	OPS [$PM_{2.5}$] (m) [0.3–2.5 μm]	*21.0* *−75.3* *−46.9*
	ME (FFF)	Classroom	• i3 MK3S (Prusa Research) • Printer (open frame) enclosed in PMMA box with doors (non-airtight) • ABS filament • PLA filament • PETG filament	• Ventilated enclosure (retrofit) – full enclosure w/LEV	OPS [PM_{10}] (m) [0.3–10 μm]	*17.7* *−76.6* *−45.1*
	ME (FFF)	Classroom	• i3 MK3S (Prusa Research) • Printer (open frame) enclosed in PMMA box with doors (non-airtight) • ABS filament • PLA filament • PETG filament	• Ventilated enclosure (retrofit) – full enclosure w/LEV	OPS [$PM_{2.5}$] (m) [0.3–2.5 μm]	*27.4* *−62.7* *−21.8*
Wojtyła, Śpiewak, and Baran (2020)	ME (FFF)	Test chamber	• Accura Genius 3D (3DKreatorUSA) • Printer (fully enclosed, non-airtight) in glass box • HIPS filament	• Isolation (retrofit) – graphitic carbon nitride-antimony doped PCO filter placed inside glass box	GC (m) Styrene Ethylbenz.	 *87*‡ *73*‡

Citation	Process[a]	Setting	Details[b]	Control[c]	Metric[d]	Efficacy (%)[e]
					Cumene	*86*[‡]
Cao et al. (2019)	ME (FFF)	Test chamber	• Up+2 (Beijing Tiertime) • Printer (open frame) placed in PMMA box (airtightness not specified) • ABS filament	• Isolation (retrofit) – full enclosure with poly-acrylonitrile nanofiber filter	Haze Detector[$PM_{2.5}$] (m)[−][*]	81.2
Davis et al. (2019)	ME (FFF)	Test chamber	• Unspecified model/manufacturer • Side walls and non-airtight hinged cover • ABS filament	• Ventilated enclosure (by design) – fully enclosed machine w/recirculating HEPA filter	TD tube (m):TVOC	−18.0
Gu et al. (2019)	ME (FFF)	Test chamber	• M200 (Zortrax) • Printer (side walls but open top) with after-market filter cover designed to seal M200 (airtightness not specified) machine • ABS filament	• Ventilated enclosure (retrofit) – full enclosure w/LEV and HEPA-ACF	FMPS (#)[5.6–560 nm]	93
					FMPS (sa)[5.6–560 nm]	93
					TD tube (m): Σ(VOCs)[&]	−16
					Ethylbenz.	100
					Styrene	15
	ME (FFF)	Test chamber	• M200 (Zortrax) • Side walls but open top • ABS filament	• Ventilation (retrofit) – air purifier w/“AntiSMOKE filter” (HEPA-ACF) at medium flow rate positioned near printer	FMPS (#)[5.6–560 nm]	89
					FMPS (sa)[5.6–560 nm]	92
					TD tube (m):Σ(VOCs)[&]	71
					Ethylbenz.	100
					Styrene	70
	ME (FFF)	Test chamber	• M200 (Zortrax) • Side walls but open top • ABS filament	• Ventilation (retrofit) – air purifier w/“AntiSMOKE filter” (HEPA-ACF) at maximum flow rate positioned near printer	FMPS (#)[5.6–560 nm]	87
					FMPS (sa)[5.6–560 nm]	91
					TD tube (m):Σ(VOCs)[&]	69
					Ethylbenz.	100
					Styrene	70

Citation	Process[a]	Setting	Details[b]	Control[c]	Metric[d]	Efficacy (%)[e]
	ME (FFF)	Test chamber	• M200 (Zortrax) • Side walls but open top • ABS filament	• Ventilation (retrofit) – air purifier w/HEPA-HIMOP at medium flow rate positioned near printer	FMPS (#)[5.6–560 nm]	74
					FMPS (sa)[5.6–560 nm]	79
					TD tube (m):Σ(VOCs)[&]	−736
					Ethylbenz.	−13[ǂ]
					Styrene	−90[ǂ]
	ME (FFF)	Test chamber	• M200 (Zortrax) • Side walls but open top • ABS filament	• Ventilation (retrofit) – air purifier w/HEPA-HIMOP at maximum flowrate positioned near printer	FMPS (#)[5.6–560 nm]	90
					FMPS (sa)[5.6–560 nm]	92
					TD tube (m):Σ(VOCs)[&]	−479
					Ethylbenz.	−33[ǂ]
					Styrene	−200[ǂ]
HSE (2019)	ME (FFF)	Test chamber	• Kora Midi (Kora) • Printer (open frame) enclosed in PMMA box • ABS filament	• Ventilated enclosure (retrofit) – full enclosure w/LEV and HEPA-ACF	DC (#)[10–300 nm]	97.0
	ME (FFF)	test chamber	• Kora Midi (Kora) • Printer (open frame) enclosed in PMMA box (air-tight) • ABS filament	• Ventilated enclosure (retrofit) – full enclosure w/LEV and recirculating HEPA-ACF	DC (#)[10–300 nm]	99.4
Oberbek et al. (2019)	ME (FFF)	Lab room	• Unspecified model/manufacturer • Printer placed in half-enclosed box (unspecified material) • Polymer (unspecified) w/HA	• Isolation (retrofit) – partial enclosure	DC (sa) [10–300 nm]	*−34.7*
					DC (#) [10–300 nm]	*−100.9*
Stefaniak et al. (2019a)	MJ	Workplace	• Objet 350 (Stratasys) • Hinged cover (non-airtight)	• Isolation (by design) – fully enclosed machine	CNC (#) [10–1000 nm]	*76.1 to 93.5*
					OPS (#) [0.3–20 μm]	*90.0 to 92.3*

Citation	Process[a]	Setting	Details[b]	Control[c]	Metric[d]	Efficacy (%)[e]
			• Support 705, TangoBlack+, VeroClear resins		PID (TVOC)	*−60.7 to 10.7*
Stefaniak et al. (2019b)	ME (FFF)	Office	• UpBox+ (Beijing Tiertime) • Side walls and non-airtight cover • ABS filament	• Ventilated enclosure (by design) – fully enclosed machine w/recirculating HEPA-ACF	CNC (#) [20–1000 nm]	*79.0*
	ME (FFF)	Workplace	• X-one (Ruian Qidi Technology Co.) • 10 printers (side walls and non-airtight cover) on shelving enclosed using PMMA panels • PLA filament	• Ventilated enclosure (retrofit) – full enclosure w/LEV and HEPA-ACF	CNC (#) [20–1000 nm] SMPS (#) [10–420 nm] PID (TVOC)	*99.7* *99.7* *53.2*
Du Preez et al. (2018)	ME (FFF)	Office/Workplace	• UpMini (Beijing Tiertime) • Side walls and non-airtight cover • ABS filament – black • PLA filament – green • ABS filament – blue • PLA filament – light blue	• Isolation (by design) – fully enclosed machine	CNC (#) [7–1000 nm] CNC (#) [7–1000 nm] CNC (#) [7–1000 nm] CNC (#) [7–1000 nm]	*88.3 to 90.1* *6.0 to 34.1* *32.9 to 39.0* *12.0 to 23.1*
	ME (FFF)	Office/Workplace	• UpBox+ (Beijing Tiertime) • Side walls and non-airtight cover • PLA filament – red	• Ventilated enclosure (by design) – fully enclosed machine w/recirculating HEPA-ACF	CNC (#) [7–1000 nm]	*42.1 to 52.6*
Yang and Li (2018)	VP (SLA)	Lab room	• Perfactory Micro EDU (EnvisionTec) • Side walls and non-airtight hinged cover • e-shell 600, LS 600 M resins	• Isolation (by design) – fully enclosed machine	PID (TVOC)	−4.6*[B]*
	VP (SLA)	Lab room	• Perfactory Micro EDU (EnvisionTec) • Side walls and non-airtight hinged cover • e-shell 600, LS 600 M resins	• Isolation (by design) – fully enclosed machine w/TiO_2 PCO in build chamber	PID (TVOC)	53.8*[B]*
	VP (SLA)	Lab room	• Perfactory Micro EDU (EnvisionTec) • Side walls and non-airtight hinged cover • e-shell 600, LS 600 M resins	• Isolation (by design) – fully enclosure machine w/activated	PID (TVOC)	72.2*[B]*

Citation	Process[a]	Setting	Details[b]	Control[c]	Metric[d]	Efficacy (%)[e]
				carbon adsorbent in build chamber		
Azimi et al. (2016)	ME (FFF)	Test chamber	• Replicator 2x (MakerBot) • Side walls and non-airtight cover • ABS filament	• Isolation (by design) – fully enclosed machine	CNC (#) [10–1000 nm]	35
					TD tube (m): Styrene	*−51.8*
					Acetoph.	*−39.0*
					I. palmitate	*32.7*
					Ethylbenz.	*−52.2*
					HTSx	*−54.4*
					N-PBE	*−48.6*
Kwon et al. (2017)	ME (FFF)	Test chamber	• 3DISON multi 2 (Rokit) • Side walls† • ABS filament	• Ventilation (retrofit) – extruder nozzle suction fan w/ACF	SMPS (#) [10–420 nm]	−38.9
	ME (FFF)	Test chamber	• 3DISON multi 2 (Rokit) • Printer (side walls†) enclosed in box (unspecified material) • ABS filament	• Ventilated enclosure (retrofit) – full enclosure w/LEV	SMPS (#) [10–420 nm]	74.4
	ME (FFF)	Test chamber	• 3DISON multi 2 (Rokit) • Printer (side walls†) enclosed in box (unspecified material) • ABS filament	• Ventilated enclosure (retrofit) – full enclosure w/LEV and ACF w/ nozzle suction fan	SMPS (#) [10–420 nm]	90.7
	ME (FFF)	Test chamber	• 3DISON multi 2 (Rokit) • Printer (side walls†) enclosed in box (unspecified material) • ABS filament	• Ventilated enclosure (retrofit) – full enclosure w/LEV and ACF	SMPS (#) [10–420 nm]	94.3
	ME (FFF)	Test chamber	• 3DISON multi 2 (Rokit) • Printer (side walls†) enclosed in box (unspecified material) • ABS filament	• Ventilated enclosure (retrofit) – full enclosure w/LEV and combination electret and antibacterial filter	SMPS (#) [10–420 nm]	76.0

Citation	Process[a]	Setting	Details[b]	Control[c]	Metric[d]	Efficacy (%)[e]
	ME (FFF)	Test chamber	• 3DISON multi 2 (Rokit) • Printer (side walls†) enclosed in box (unspecified material) • ABS filament	• Ventilated enclosure (retrofit) – full enclosure w/LEV and polyethylene filter	SMPS (#) [10–420 nm]	92.9
	ME (FFF)	Test chamber	• 3DISON multi 2 (Rokit) • Printer (side walls†) enclosed in box (unspecified material) • ABS filament	• Ventilated enclosure (retrofit) – full enclosure w/LEV and nanomembrane filter	SMPS (#) [10–420 nm]	95.7
	ME (FFF)	Test chamber	• 3DISON multi 2 (Rokit) • Printer (side walls†) enclosed in box (unspecified material) • ABS filament	• Ventilated enclosure (retrofit) – full enclosure w/LEV and HEPA filter	SMPS (#) [10–420 nm]	99.9
	ME (FFF)	Test chamber	• 3DISON multi 2 (Rokit) • Printer (side walls†) enclosed in box (unspecified material) • HIPS filament	• Ventilated enclosure (retrofit) – full enclosure w/LEV and HEPA filter	SMPS (#) [10–420 nm]	99.9
Stefaniak et al. (2017b)	ME (FFF)	Test chamber	• Replicator 2x (MakerBot) • Side walls and non-airtight cover • ABS, PLA filaments	• Isolation (by design) – fully enclosed machine	PID (TVOC) Canister (m): IPA Ethylbenz. Styrene	*−3.6*[B] *70.7*[B] *76.2*[B] *36.9*[B]
Zontek et al. (2017)	ME (FFF)	Lab room	• da Vinci 1.03D (XYZprinting) • Side walls, top, and hinged non-airtight door • ABS filament	• Isolation (by design) – fully enclosed machine	SMPS (#) [2–300 nm] SMPS (m) [2–300 nm]	94.7 99.9
Yi et al. (2016)	ME (FFF)	Test chamber	• Replicator 2x (MakerBot) • Side walls and non-airtight cover • ABS filament	• Isolation (by design) – fully enclosed machine	SMPS (#) [15–660 nm] CNC (#) [20–1000 nm] ELPI (#) [24–9380 nm]	*47.2*[B] *58.2*[B] *67.9*[B]

Citation	Process[a]	Setting	Details[b]	Control[c]	Metric[d]	Efficacy (%)[e]
					OPS (#) [0.3–20 μm]	*45.1* [B]
	ME (FFF)	Office	• Replicator 2x (MakerBot) • Side walls and non-airtight cover • ABS filament	• Isolation (by design) – fully enclosed machine	SMPS (#) [10–360 nm]	*73.7* [B]
Administrative						
Stefaniak et al. (2022)	ME (FFF) – granulating waste plastic task	Lab room	• Commercial shredder • Waste PLA prints	• Distance (1.8 m from shredder)	APS (#) [0.5–20 μm]	*79.8* [B]
					OPS (#) [0.3–10 μm]	*27.3* [B]
					CNC (#) [20–1000 nm]	*68.9* [B]
					PID (TVOC)	*65.2* [B]
	ME (FFF) – granulating waste plastic task	Lab room	• Commercial shredder • Waste ABS prints	• Distance (1.8 m from shredder)	APS (#) [0.5–20 μm]	*−250.7* [B]
					OPS (#) [0.3–10 μm]	*−166.7* [B]
					CNC (#) [20–1000 nm]	*−62.4* [B]
					PID (TVOC)	*−11,700.0* [B]
	ME (FFF) – filament making task	Lab room	• Commercial filament extruder • Rough and final extrusions • Waste PLA granules	• Distance (1.2 m from extruder)	CNC (#) [20–1000 nm]	*−32.8 to 70.7* [B]
					PID (TVOC)	*76.1 to 81.1* [B]
	ME (FFF) – filament making task	Lab room	• Commercial filament extruder • Rough and final extrusions • Waste ABS granules	• Distance (1.2 m from extruder)	CNC (#) [20–1000 nm]	*−233.5 to 43.3* [B]
					PID (TVOC)	*80.5 to 93.5* [B]
	ME (FFF) – filament making task	Lab room	• Commercial filament extruder • Final extrusion • Virgin PLA, ABS, HDPE, LDPE, HIPS, or PP pellets	• Distance (1.2 m from extruder)	PID (TVOC)	*−324.1 to 84.8* [B]

Citation	Process[a]	Setting	Details[b]	Control[c]	Metric[d]	Efficacy (%)[e]
	ME (FFF) – filament making task	Lab room	• Commercial filament extruder • Final extrusion • Virgin ABS, HDPE, LDPE, or HIPS pellets	• Distance (1.2 m from extruder)	APS (#) [0.5–20 μm]	*87.2 to 97.3 [B]*
	ME (FFF)	Lab room	• Unspecified model/manufacturer • Open frame • Recycled PLA, recycled ABS, or virgin ABS filaments	• Distance (2.4 m from printer)	PID (TVOC)	*63.8 to 88.5 [B]*
	ME (FFF)	Lab room	• Unspecified model/manufacturer • Open frame • Recycled PLA, virgin ABS, virgin HDPE, virgin LDPE, or virgin HIPS filaments	• Distance (2.4 m from printer)	APS (#) [0.5–20 μm]	*−131.4 to 99.9 [B]*
Han, Zhao, and Li (2021)	VP (SLA) – resin mixing pre-printing task	Lab room	• Mixed resin ingredients at two different speeds	• Reduced stirring speed from 500 rpm to 250 rpm	PID (TVOC)	*9.5*
	Shape programming post-processing task	Lab room	• Thermally stimulated shape programming using two approaches	• Used water bath rather than hotplate	PID (TVOC)	*88* ‡
	Shape programming post-processing task	Lab room	• Thermally stimulated shape programming using two temperatures	• Decreased water bath from 62 C to 52 C	PID (TVOC)	*39* ‡
	Shape recovery post-processing task	Lab room	• Thermally stimulated shape recovery using two temperatures	• Decreased water bath from 62 C to 52 C	PID (TVOC)	*39* ‡
Khaki et al. (2021)	ME (FFF)	Private home	• Ender 3 (Creality) • Open frame • ABS filament	• Warning sensor for particles based on low-cost indoor air quality monitor	OPS (#) [0.3–10 μm]	Precise[f]

Citation	Process[a]	Setting	Details[b]	Control[c]	Metric[d]	Efficacy (%)[e]
Wojnowski et al. (2020)	ME (FFF)	Test chamber	• Prusa i3 MK2S (Prusa Research) • Open frame • ABS filament	• Warning sensor for BTEX based on low-cost electrochemical sensors	EC sensor	Accurate[g]
Bau et al. (2020)	DED	Workplace	• Magic800 (BeAM) • Sealed machine doors • Stainless-steel 316 and Inconel 625 powders	• Time-delay to open sealed machine w/LEV	Time	8 min
HSE (2019)	ME (FFF)	Test chamber	• Kora Midi (Kora) • Printer (open frame) enclosed in PMMA box • ABS filament	• Time-delay to open retrofit full enclosure w/LEV and HEPA filter	Time	20 min[B]
	ME (FFF)	test chamber	• Kora Midi (Kora) • Printer (open frame) enclosed in PMMA box (air-tight) • ABS filament	• Time-delay to open retrofit full enclosure w/LEV and recirculating HEPA filter	Time	20 min[B]
Lewinski, Secondo, and Ferri (2019)	BJ	Lab room	• R1 (ExOne) • Fully enclosed (non-airtight) • Stainless-steel powder	• Distance (3 m from printer)	CFC (m)	*75.0*[B]
Stefaniak et al. (2019b)	ME (FFF)	Workplace	• X-one (Ruian Qidi Technology Co.) • 10 printers (side walls and non-airtight cover) on shelving enclosed using PMMA panels • PLA filament	• Time-delay to open retrofit full enclosure w/LEV and HEPA-ACF	Time	30 min
Cheng et al. (2018)	ME (FFF)	Test chamber	• Creator 3 (Flashforge) • Fully enclosed (non-airtight) • ABS filament	• Varied infill heights, densities, and patterns; filament feed rate of the first top layer	OPS (#) [0.3–25 μm]	96
Simon et al. (2018)	ME (FFF)	Clean room	• Ultimate 3D Printer (Monoprice) • Open frame[//]	• Increased print speed from 25% to 150% of default	SMPS (#) [10–420 nm]	*−280.0*

Citation	Process[a]	Setting	Details[b]	Control[c]	Metric[d]	Efficacy (%)[e]
			• ABS filament			
	ME (FFF)	Clean room	• Ultimate 3D Printer (Monoprice) • Open frame[//] • ABS filament	• Pre-cleaned extruder nozzle	SMPS (#) [10–420 nm]	*100.0*
Deng et al. (2016)	ME (FFF)	Clean room	• Creator 3 (Flashforge) • Fully enclosed (non-airtight) • ABS filament	• Retract filament from extruder nozzle during pre-heating	CNC (#) [2.5–3000 nm]	75
Zhou et al. (2015)	ME (FFF)	Clean room	• Measured emissions in NF and FF (unspecified model/manufacturer) • Open frame • ABS filament	• Distance (1.8 m from one printer)	OPS (#) [0.25–32 μm]	*−50*[≠]
	ME (FFF)	Clean room	• Measured emissions in NF and FF (unspecified model/manufacturer) • Open frame • ABS filament	• Distance (4 m from one printer)	OPS (#) [0.25–32 μm]	*−83*[≠]
	ME (FFF)	Clean room	• Measured emissions in NF and FF (unspecified model/manufacturer) • Open frame • ABS filament	• Distance (1.8 m from two printers)	OPS (#) [0.25–32 μm]	*−419*[≠]
	ME (FFF)	Clean room	• Measured emissions in NF and FF (unspecified model/manufacturer) • Open frame • ABS filament	• Time-delay to open clean room w/LEV (90 ACH) after operating one printer	Time	10 min[*[B]*]
	ME (FFF)	Clean room	• Measured emissions in NF and FF (unspecified model/manufacturer) • Open frame • ABS filament	• Time-delay to open clean room w/LEV (90 ACH) after operating two printers	Time	40 min[*[B]*]
Personal protective equipment						

Citation	Process[a]	Setting	Details[b]	Control[c]	Metric[d]	Efficacy (%)[e]
Graff et al. (2017)	PBF (SLM)	Workplace	• Model SR500 respiratory protection (Sundström)	• Powered air-purifying respirator	OPS (m) [0.3–10 μm]	>99[ǂ]

[a] BJ = binder jetting, DED = directed energy deposition, FDM™ = fused deposition modeling, FFF = fused filament fabrication, LFAM = large format additive manufacturing, ME = material extrusion, MJ = material jetting, PBF = powder bed fusion, SLA = stereolithography, SLM = selective laser melting, VP = vat photopolymerization

[b] ABS = acrylonitrile butadiene styrene, HA = hydroxyapatite, HDPE = high density polyethylene, HIPS = high impact polystyrene, LDPE = low density polyethylene, PC = polycarbonate, PEOT/PBT = poly(ethylene oxide) terephthalate/poly(butylene terephthalate), PET-CF = polyethylene terephthalate-carbon fiber reinforced, PETG = PET (glycol-modified), PLA = polylactic acid, PMMA = poly(methyl methacrylate), PP = polypropylene, PPS = polyphenylene sulfide, PSU = polysulfone, rGO = reduced graphene oxide, TPU = thermoplastic polyurethane

[c] ACF = activated charcoal filter, ACH = air change per hour, BTEX = benzene, toluene, ethylbenzene, and xylenes, CFD = computational fluid dynamics, GEV = general exhaust ventilation, HEPA = high-efficiency particulate air, HIMOP = high-efficiency multi-oxidation pottery and porcelain granule, LEV = local exhaust ventilation, PCO = photo catalytic oxidation, rpm = rotations per minute, TiO_2 = titanium dioxide

[d] Acetald. = acetaldehyde, Acetophen. = acetophenone, Benzald. = benzaldehyde, Butyrald. = butyraldehyde, CFC = close-faced 37-mm cassette, CNC = condensation nuclei counter, DC = diffusion charger, EC = electrochemical, ELPI = electrical low-pressure impactor, Ethylbenz. = ethylbenzene, FMPS = fast mobility particle sizer, Formald. = formaldehyde, GC = gas chromatography, Hexald. = hexaldehyde, HTSx. = hexamethyl cyclotrisiloxane, IPA = isopropyl alcohol, I. palmitate = isopropyl palmitate, Isob. acrylate = isobornyl acrylate, m = mass-based particle or gas measurement, m-AMS = mini-aerosol mass spectrometer, *N*-PBE = N-[(pentafl) benzene ethanamine, OPS = optical particle sizer, PID = photoionization detector, PM_X = particulate matter with aerodynamic diameter less than 2.5 or 10 μm, Propionald. = propionaldehyde, Prop. glycol = propylene glycol, sa = surface area-based particle measurement, SMPS = scanning mobility particle sizer, TC = thermal cycle, TD tube = thermal desorption tube, TVOC = total volatile organic compounds, # = number-based particle measurement

[e] negative sign (−) = contaminant level increased in air when control was in place; time-delay administrative controls, unit is minutes (min) for emission levels to return to background concentration

[f] Precise = low-cost indoor air quality sensor recorded consistent particulate matter profiles with research-grade aerosol monitor for each print test

[g] Accurate = array of low-cost electrochemical sensors had 0.96 classification accuracy to correctly determine that a predetermined threshold concentration for BTEX compounds was exceeded as compared with proton transfer reaction mass spectrometry; n/a = not applicable

[ǂ] Value estimated from plots of data

[∩] Specific filament(s) that correspond to reduction value were not specified

[*B*] = efficacy calculated as change relative to background contaminant level

[!!] Full ventilated enclosure but LEV off for testing

[*] Instrument size range not reported

[&] ΣVOCs = identified and unidentified substances eluting between (and including) n-hexane and n-hexadecane

[†] Non-airtight full enclosure design by manufacturer but front door and cover removed for testing

[//] Open frame design by manufacturer but all sides covered with polycarbonate panels for testing (airtightness not specified)